

NASA TM-112649



Validation of a Deterministic Vibroacoustic Response Prediction Model

*Raoul E. Caimi
NASA DM-ASD
John F. Kennedy Space Center, Florida*

*Ravi Margasahayam
I-NET Space Services
John F. Kennedy Space Center, Florida*

National Aeronautics and Space Administration
John F. Kennedy Space Center, Kennedy Space Center, Florida 32899-0001

April 1997

TABLE OF CONTENTS

<u>Section</u>	<u>Title</u>	<u>Page</u>
1.	INTRODUCTION	1
2.	BACKGROUND	4
3.	VERIFICATION TEST ARTICLE (VETA)	6
3.1	VETA Conceptual Design	6
3.2	VETA Launch Pad Siting Issues	7
3.3	VETA Instrumentation	8
3.3.1	Launch-Induced Acoustic Loads	8
3.3.2	Strain Response	9
3.3.3	Acceleration Response	10
3.3.4	Data Acquisition System (DAS)	10
4.	STRUCTURAL DYNAMICS	11
4.1	Relationship Between Mode Shape and Stress	11
4.2	Dependence of Natural Frequency on Material, Geometry, and Support.....	12
5.	FIELD TESTS	12
5.1	Modal Tests	12
5.2	Dynamic Tests.....	14
6.	ANALYSIS METHODOLOGY	14
6.1	Load Characterization	16
6.2	Analysis Using the C-Beam Program	16
6.3	Response Characterization	17
7.	ANALYSIS-TEST CORRELATION	18
7.1	Correlation Procedure.....	19
7.2	General Observations	20
7.3	Correlation Results	21

TABLE OF CONTENTS (cont)

<u>Section</u>	<u>Title</u>	<u>Page</u>
8.	CONCLUSIONS	21
9.	BIBLIOGRAPHY	22
APPENDIX A	VETA DESIGN DETAILS	A-1
APPENDIX B	DATA ACQUISITION SYSTEM	B-1
APPENDIX C	ACOUSTIC LOAD DEFINITION	C-1
APPENDIX D	C-BEAM PROGRAM OUTPUT.....	D-1
APPENDIX E	STRUCTURAL RESPONSE	E-1
APPENDIX F	TEST ANALYSIS CORRELATION	F-1

LIST OF FIGURES

<u>Figure</u>	<u>Title</u>	<u>Page</u>
1	VETA Program Flowchart	3
2	Input Pressures and Response Strain Amplitude Probability Distributions Depicting Non-Gaussian Distribution	5

LIST OF TABLES

<u>Table</u>	<u>Title</u>	<u>Page</u>
1	VETA Database for Launch Pads 39A and 39B Launches	2
2	Vibration in Flexure	13
3	Comparison of Flexural Natural Frequencies [Theoretical (C-BEAM) Versus Modal and Dynamic Tests]	15
4	Near-Field Acoustic Database.....	15

ABBREVIATIONS AND ACRONYMS

A/D	analog to digital
COH	coherence
CP	Centaur Porch
CPD	correlated pressure distribution
CPSD	cross-power spectral density
DAS	data acquisition system
DAT	digital audio tape
GMT	Greenwich Mean Time
GSE	ground support equipment
Hz	hertz
J	joint acceptance
KSC	John F. Kennedy Space Center
KSDN	Kennedy Space Center Data Network
OWPS	Orbiter Weather Protection Structure
p(+)	acoustic pressure
PCL	pressure correlation length
PHA	phase
PSD	power spectral density
PTCR	Pad Terminal Connection Room
RS	response spectra
RMS	root mean square
SPL	sound pressure level
STS	Space Transportation System
T-0	launch minus zero minutes and seconds
VETA	Verification Test Article
°F	degree Fahrenheit

VALIDATION OF A DETERMINISTIC RESPONSE PREDICTION MODEL

1. INTRODUCTION

During the launch of a Space Shuttle, ground support equipment and structures in the proximity of the launch pad (within 300 feet) are often exposed to intense vibration due to acoustic pressure loads generated by rocket exhausts. The term vibroacoustics or vibroacoustic coupling is a measure of a structure's affinity to vibrate when subjected to broadband acoustic loads leading to degradation of structures and, thereby, increasing safety concerns and operational maintenance costs. Thus, continuous monitoring of launch-critical loads (acoustics) and structural response (vibration and strain) is vital for ensuring operational safety and long-term reliability of launch pad structures.

The scope of this study included the processing of selected measurements from Shuttle launches within the launch pad perimeter, verification of the deterministic approach via computation of response spectra (RS), and validation of the concept of an equivalent load. These computations will be used by engineers and structural designers to set guidelines for preliminary design and dynamic tests. The study covered a time span beginning with the STS-59 launch on April 9, 1994, and ended with STS-74 launch on November 12, 1995 (see table 1). Appendices A through E contain supporting figures, computations, and data. The development of deterministic concepts is covered in published documents (see the references in section 9, items a through g).

Past efforts at the John F. Kennedy Space Center (KSC) have focused on the development of analytical tools both to characterize noise and to predict vibratory response of structures during launch. Two analytical models (probabilistic and deterministic) for solving random vibration problems have been proposed. The choice of a solution model was governed by observations drawn from simultaneous acoustics and vibration response measurements during the launch of a Shuttle and the accuracy with which each model predicts low-frequency (0 to 50 hertz) vibration response. The most appropriate model will aid in optimizing the design of new and support modifications of existing structures.

Figure 1 depicts the overall effort required for designing a structure, exposing it to the Shuttle launch environment, comparing the analytically predicted responses to those measured, and validating the deterministic approach. Space system launch vehicles present the most severe random-vibration environment to which the ground support equipment (GSE) is exposed. Since this type of environment is

Table 1. VETA Database for Launch Pads 39A and 39B Launches

Parameters	Launch Number					
	STS-59	STS-65	STS-64	STS-68	STS-66	STS-63
Date	9-Apr-94	8-Jul-94	9-Sep-94	30-Sep-94	3-Nov-94	3-Feb-95
T-0 (GMT)	11:05:00	16:43:00	22:22:55	11:16:00	16:59:43	05:22:04
Launch Pad	A	A	B	A	B	B
MLP	2	3	2	1	3	2
Wind Speed (knots)	17	8	9	11	9	10
Wind Direction (degrees)	99	107	115	68	66	238
Relative Humidity (%)	74	76	71	71	64	83
Temperature (°F)	72	84	83	79	76	55
Orbit (degree inclination)	57	28.45	57	57	57	51.6

Parameters	Launch Number				
	STS-67	STS-71	STS-70	STS-69	STS-74
Date	2-Mar-95	27-Jun-95	13-Jul-95	7-Sep-95	12-Nov-95
T-0 (GMT)	06:38:13	19:32:19	13:41:55	11:09:00	07:30:43
Launch Pad	A	A	B	A	A
MLP	1	3	2	1	--
Wind Speed (knots)	10	8	5	--	6.7
Wind Direction (degrees)	273	76	43	--	289
Relative Humidity (%)	87	82	79	--	82
Temperature (°F)	64	85	83	--	50
Orbit (degree inclination)	28.45	51.6	28.45	28.4	51.6

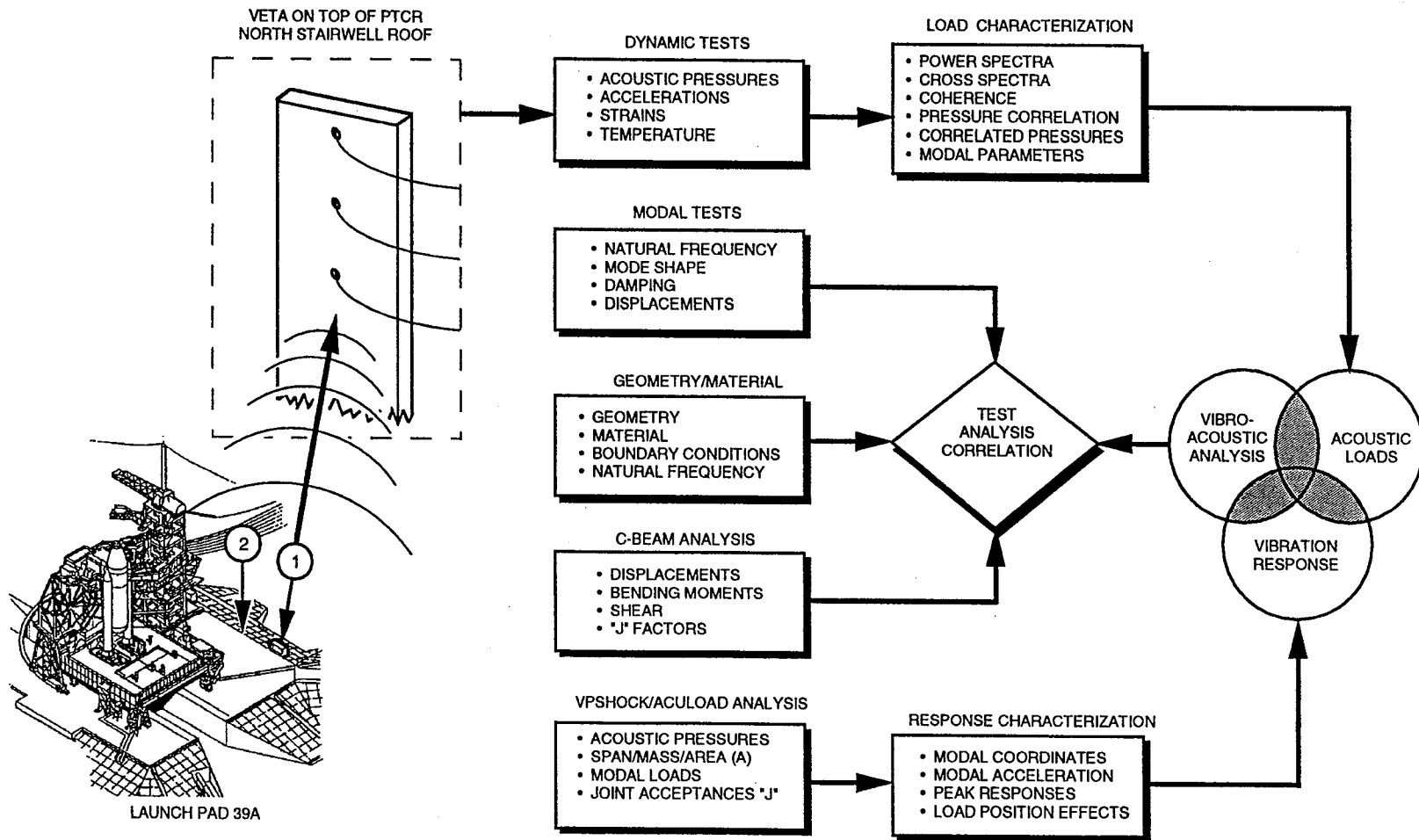


Figure 1. VETA Program Flowchart

difficult to reproduce in a laboratory, data gathered from field tests is the only avenue for test analysis correlation.

2. BACKGROUND

The design of launch pad structures, particularly those having a large area-to-mass ratio, is governed by launch-induced acoustic pressures, which are relatively short transient with random amplitudes and a non-Gaussian distribution (see figure 2, which also includes cumulative probabilities computed from plotted probability densities. The factors influencing acoustic excitation and the resulting structural response are numerous and cannot be predicted precisely. This poses a dilemma for ground facility and GSE designers since they must use sophisticated dynamic analysis methods to incorporate the effect of launch-induced acoustic loads or exclude these effects in total.

Decade-long research at KSC has focused on accurate field measurements and the subsequent characterization of launch acoustic loads. This research led to the development of a deterministic approach to accurately predict the random vibration response of structures (see references in section 9, items d through g). The deterministic approach can be used to state the launch-induced acoustics as a "static equivalent load" by computing an acoustic pressure response spectra, which is familiar to GSE designers. The purpose of this report entails verification of the deterministic approach using a launch-pad-installed cantilever beam by comparing predicted and measured strains.

A cantilever beam was used to assess accuracy and limitations, if any, of a deterministic approach to predict the response of launch pad structures exposed to Space Shuttle launch-induced acoustic excitation. It was carefully designed so the fundamental natural frequency of the flexural mode was approximately 8.9 hertz, since this frequency lies within the range of natural frequencies (0 to 20 hertz) of major launch pad structures of interest in the near-field (0 to 300 feet).

The vibration mode with the lowest frequency (often called the fundamental natural frequency or sometimes the resonant natural frequency) usually has the simplest mode shape, the largest amplitudes of structural distortion and stress, and the fewest nodes (points of zero displacement). Since the fundamental natural frequency (which has the greatest displacements and stresses) is the one that usually becomes easily excited, it is the one of primary concern. Higher frequencies corresponding to higher modes of vibration are of less interest since their contribution to the overall vibration is often lower, assuming they become excited at all during tests. For analysis purposes, the first four flexural (bending) modes of vibration were computed, but only the first mode was used for test-analysis correlation since launch trajectory significantly affected correlation.

SHUTTLE-RSRM, Relations between INPUT and RESPONSE Amplitude Distributions on FSS.

R-RANGE (-/+)-SIGMAS 1 0.50 0.75 1.00 1.25 1.50 1.75 2.00 2.25 2.50 2.75 3.00

MPD27a PROBL-R(X/R)1 0.4747 0.6577 0.8814 0.9325 0.9612 0.9765 0.9855 0.9900 0.9940 0.9970

MPD27b PROBL-R(X/R)1 0.6648 0.8062 0.8881 0.9371 0.9650 0.9798 0.9883 0.9934 0.9966 0.9982 0.9992

RESPONSE MPG27a 1 0.6057 0.7551 0.8520 0.9120 0.9511 0.9737 0.9865 0.9931 0.9972 0.9989 0.9995

Table of cumulative probabilities (Prob: Integrate) computed from plotted probability densities.

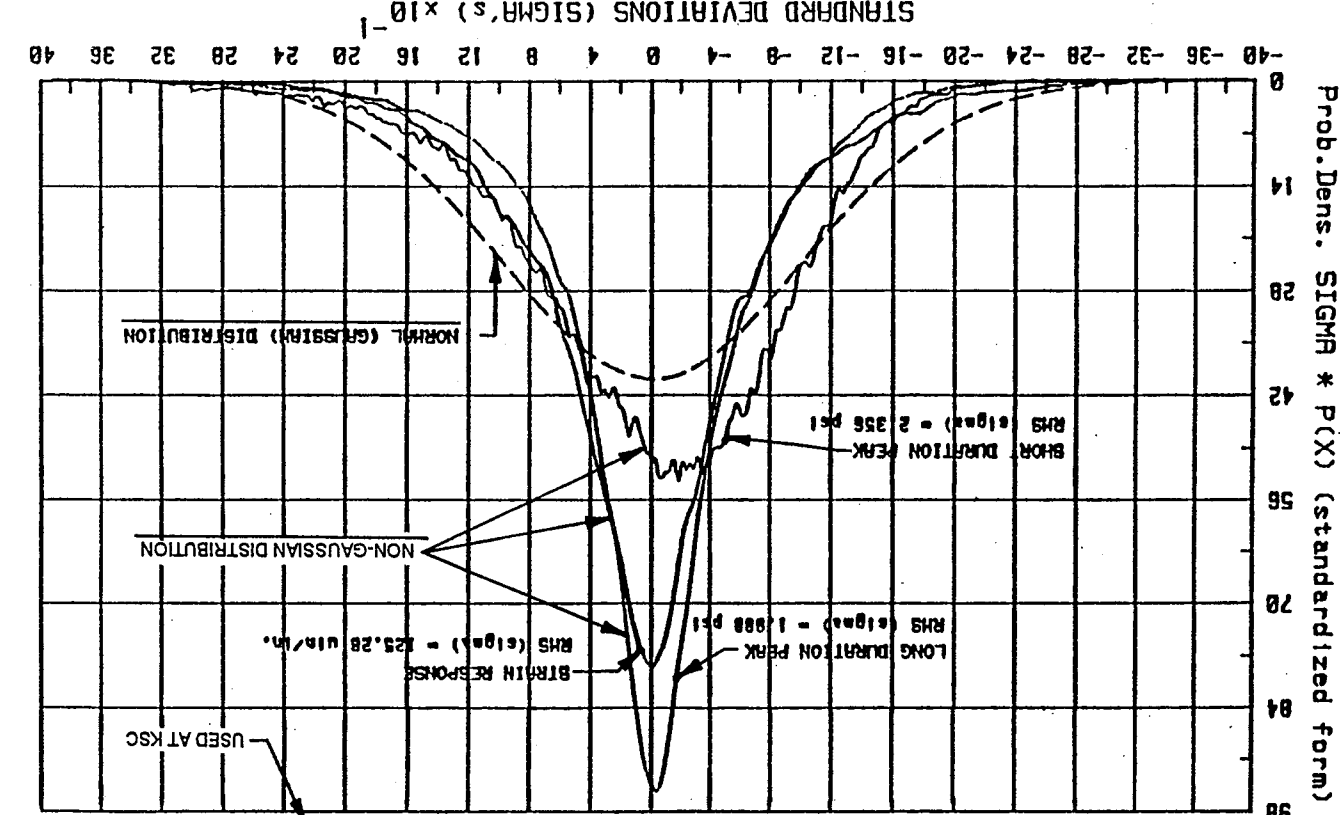


Figure 2. Input Pressures and Response Strain Amplitude Probability Distributions Depicting Non-Gaussian Distribution

MPG27a Problems. BOEING Aerospace Operations

Past results indicated the predictions are favorable especially in the low frequency range (0 to 50 hertz). Use of the static equivalent launch acoustic load approach was validated for the first mode. However, additional tests were necessary to enhance confidence in the deterministic approach, higher modes, and varying launch pad azimuth locations and to improve prediction accuracies.

3. VERIFICATION TEST ARTICLE (VETA)

3.1 VETA CONCEPTUAL DESIGN

The VETA project represents the first comprehensive effort to design a safe structure, install it within the launch pad perimeter, and measure acoustic and vibration response data simultaneously. To aid test analysis correlation efforts, the following special test requirements were established prior to the design:

- a. Simple in design
- b. Ease of manufacture
- c. Installation provisions for sensors
- d. Well-defined local boundary conditions
- e. Provision for sufficient surface area for excitation
- f. Orientation to provide adequate excitation
- g. Careful siting leading to peak stresses of at least half the material yield
- h. First fundamental mode of approximately 10 hertz
- i. Measurable strain signal for cable lengths used (250 to 350 feet)
- j. Simultaneous and correct phasing of measured parameters
- k. No influence on any aspect of ongoing Shuttle operations
- l. Capability to remotely monitor the measurement parameters

A total of four unique designs were considered and analyzed prior to the selection of a cantilever-type structure. Simplicity and the ability to characterize the structure

analytically even prior to the test led to the choice of a cantilever beam as the VETA. Appendix A includes several elevations and cross-sectional details of the VETA (see figures A-1 through A-3).

The test article was composed of a steel plate (14 by 3/16 by 127 inches) with two tee sections (WT3X4.25) welded in the shape of a cantilever beam. This assembly was in turn welded to a specially designed steel base, with provision for eight anchor bolts for launch pad installation. The test article design was typical of launch pad structures.

The test article was designed to respond primarily in flexure about its weak stiffness axis (x-x) and with a first fundamental frequency of 8.9 hertz. Most launch pad structure resonances are in the 0 to 20 hertz range, which falls within the desired range. The test article was also designed to carry an equivalent static load of approximately 2 pounds per square inch applied to a single side. An ample safety factor against effective acoustic loads at the intended location was provided. The base, when adequately anchored to the concrete foundation, was designed to withstand the ultimate load on the cantilever. The ultimate load, which produces a yield in the cantilever, only produces allowable stresses in the base under peak acoustic loading conditions. Thus, the structure bends before it breaks and, therefore, is not hazardous to launch operations.

3.2 VETA LAUNCH PAD SITING ISSUES

The test article was installed on the northwest side of Launch Pad 39A, about 240 feet diagonally from the vehicle centerline and at an azimuth of 330 degrees. Interference with normal launch pad operations was minimized by siting the test article on the top of the Pad Terminal Connection Room (PTCR) stairwell about 20 feet above the launch pad surface (see figures A-4 and A-5).

At this location, the VETA was exposed to both direct and reflected acoustics. It is important to note that the acoustic loads on GSE are location dependent to a large degree and vary when the GSE is partially or fully shielded from direct acoustics. This location constituted acoustic near-field (0 to 300 feet from the vehicle centerline) conditions, where inverse square laws of acoustic energy decay do not apply. Since most critical launch pad structures are within the 0-to-300-foot range, the chosen location closely reflected the nature of exposed acoustics on GSE.

In addition to the siting issues, acoustic loads were found to be significantly affected by vehicle trajectory governed by the mission-dependent launch inclination (see figure A-6). Rocket engine test firings conducted in the past and the conclusion derived thereof have relied heavily on stationary rocket and stationary sensor

scenarios, using horizontally mounted rockets. VETA tests, however, truly reflect the reality of the effects a moving-rocket on stationary sensors or structures, typical of GSE.

Lastly, GSE structures exposed to near-field acoustics are also subject to front and back pressures depending on the location and launch trajectory. Past analytical efforts at KSC used acoustic data from sensors mounted in the front. Once the liftoff peak was measured, this sensor was not exposed to any acoustics during the roll maneuver, which exposed the backside of the structures to a back pressure. Significant back pressures were observed during VETA tests not only during the roll maneuver but also liftoff. Depending on the launch inclination, instantaneous acoustic loads during the roll maneuver were significantly higher than during liftoff. This necessitated instrumenting the VETA both in the front and the back.

Accounting for front and back pressures explains why some structures on the launch pad have failed when others did not. Structure exposure to front and back pressures can have the net effect of lowering the acoustic load. However, in a random vibration environment, it is highly likely that the net effective load on the structure may be higher than assumed, leading to its early failure. In short, it is not only imperative that the definition of the acoustic load be correct, but the dynamic analysis methodology must also be rigorous especially in the low frequency range (0 to 20 hertz). The development and validation of the deterministic approach was prompted by these and other issues requiring accurate response prediction in the low frequency regime (0 to 50 hertz). Statistical energy analysis (SEA) methods cannot be applied in this range.

3.3 VETA INSTRUMENTATION

Accuracy of measurements associated with this test were extremely critical to test/analysis correlation and eventual verification of the deterministic method. Proper selection of transducers and transducer placement, mounting, and calibration were key to the success of the project. An overall schematic of the VETA data acquisition subsystems is contained in appendix B, figure B-1, including sensor details. Specific sensors used for measuring launch-induced acoustic loads and subsequent structural response are discussed in 3.3.1 through 3.3.3.

3.3.1 LAUNCH-INDUCED ACOUSTIC LOADS. Most GSE structures are exposed to acoustics both in the front and in the back. For analysis, knowledge of the net effective load on the structure is required rather than the measurement of the front incident pressure alone. Therefore, the test article was instrumented with six acoustic microphones (see figure A-1). Three were installed on the front face and three were installed on the rear. Both incident and reflected acoustic pressures were measured. The net effective load on the test article was determined by

computing the difference between front and back pressures. All response spectra computations were based on the net effective pressures.

The sensors were mounted at 3-foot distances along the vertical direction. This was important to understand the distribution of the load along the cantilever in the vertical direction and to compute vertical pressure correlation lengths (see 6.3). These sensors provided multiple redundancy since the launch environment is harsh and the probability of sensor failure is high.

The PCB piezotronics model 103A02, a highly sensitive microphone having high resolution, was used for the dynamic tests. These microphones had an ample dynamic range (78 to 86 decibels) and were typically used to measure transient events, turbulence, and other acoustic phenomenon where instantaneous pressures approached or exceeded 1 pound per square inch. Sensor installation details are included in figure A-3.

Launch acoustic environment data (such as plume pressures, acoustics, strains in structural members, and vibration) were random, nonstationary, and wideband in nature. Data time histories encompassing the Shuttle liftoff period starting at T-0 seconds to T+7 seconds, the clearance of the tower starting at T+7 seconds to the start of the roll maneuver at approximately T+10 seconds, and the interval between the start and the end of the roll maneuver of about 7 seconds have been used for characterization of the acoustic load. Data time histories represented long-duration transients where, in general, both the mean and the standard deviation within a short-duration interval also varied with time.

3.3.2 STRAIN RESPONSE. The measurement of strains on the test article was vital for test-analysis correlation. Four strain gages were installed at two separate locations on the tee section of the flanges (see figure A-1). The first set of strain gages was located 12 inches above the base. This section assumed uniform strain distribution across the flange and resulted in consistent strain measurements for both the gages. For the purpose of initial calibration, the expected range of peak strains was below 700 microinches per inch. General-purpose single element, self-temperature compensating strain gage model CEA-06-062UW-350 (made by Micromasurements and having a gage length of 0.25 inch and grid resistance of 350 ohms) was used.

A second set of strain gages was located close to the inflection point (the zero curvature point of the second bending mode) at 33 inches above the base and measured from the fixed end of the test article. The purpose of this set of gages was to effectively assess the contribution of individual modes (first and second) if they became excited.

Examination of strain data yields valuable information on modal coupling. Past experience with such diverse structures as the Centaur Porch (CP) and the Orbiter Weather Protection Structure (OWPS) did not disclose any merged or closely spaced peaks, indicating the modes were distinct and there was no coupling. Modal coupling commonly occurs between much higher modes than the fundamental mode, especially in the high-frequency range where modal density is also high. However, these modes seldom, if ever, govern GSE design.

3.3.3 ACCELERATION RESPONSE. Three separate accelerometers were installed on the test article. One was installed at the tip (free end) of the cantilever beam and two were installed on the tee sections about 67 inches from the fixed end. The selected accelerometers were made by Kistler and were K-shear type model 8704B50. The accelerometers' hermetically sealed titanium housing proved sufficiently rugged for measuring peak accelerations during Space Shuttle liftoff. Accelerometer output was used to identify the excited modes and compute the root mean square (RMS) displacement in peak modes. This accelerometer model was suitable for low-level, low-frequency measurements. Two accelerometers were mounted on the tee section to yield information on torsionally induced loads or to detect twisting of the VETA. In general, flexural (bending) modes were of immediate interest since flexural mode natural frequencies are much lower than those of torsional modes and consequently, the resulting stresses are usually greater (see figure A-1).

3.3.4 DATA ACQUISITION SYSTEM (DAS). A unique and innovative solution was sought to remotely monitor and record launch data. The DAS was influenced by technical, cost, operation, and management considerations. DAS requirements included:

- a. Low initial/maintenance/operational costs
- b. Remote data acquisition, control, and data transfer
- c. Timer control for night launches
- d. Capability to control multiple recorders
- e. Capability for real-time data monitoring
- f. Instant data accessibility after launch
- g. Integration into and use of existing data
- h. Rugged, flexible, transportable, and an upgrade potential

To accurately assess the Space Shuttle vibroacoustic environment, a DAS system that samples data at a high sampling rate (12 kilohertz), high dynamic range (84 decibels), high amplitude sensitivity [14 bit analog to digital (A/D)], and low phase shift between channels (less than 1 degree) was essential. In addition to a frequency resolution capability of direct current to 10 kilohertz, recorders provided a 32-fold increase in amplitude sensitivity to the existing launch pad system. TEAC digital audio tape (DAT) recorders coupled with QuikVu tape control software met the need. PcAnywhere, an off-the-shelf software, aided in point-to-point remote control capabilities and remote computer restart options. QuikVu software was customized extensively to meet project requirements with features that included control of up to seven recorders, special windows for sensor calibrations, the option to strip multiplexed data, and quick-look data plotting capabilities. TEAC DAT recorders, QuikVu software, and PcAnywhere software formed the core of the VETA DAS and is shown in figure B-1.

The recorders and their related signal conditioning hardware were safely installed 100 feet below the launch pad surface inside the concrete base. About 150 feet of cable connected the sensors on top of the launch pad surface and the DAT recorders. Additionally, a dedicated Kennedy Space Center Data Network (KSDN) line connected the recorders to a computer in an office at the NASA Headquarters Building about 10 miles away from the launch pad. This unique setup provided remote monitoring of data during launch and total control of the DAT recorders from the office. Optional features included timer/interval recording to facilitate unmanned operation.

4. STRUCTURAL DYNAMICS

VETA structural dynamic experimental program must include two important relationships: (1) a relation between the mode shape of a structure and the stress in acoustic and acceleration environments and (2) the dependency of natural frequency and mode shape of the structure on its material, geometric, and support (boundary conditions) properties.

4.1 RELATIONSHIP BETWEEN MODE SHAPE AND STRESS

The acoustic and vibration environment generated by the launch of a Space Shuttle is random, nonstationary, and composed of a broad band of frequencies. In either case, given the launch-induced environment, it is the natural frequency and mode shape of the structure that will determine the magnitude of the response

to external loads (acoustics, pressures, etc.). Moreover, if the structure is shielded or exposed to reflected acoustics, acoustic loads at certain frequencies may be much larger (amplified) or much smaller (attenuated) when arriving at the structure being analyzed. It should be noted that the deformations a structure undergoes are assumed proportional to the loads imposed on it and the stresses in the structure are related to the deformations (or strains) through the elastic moduli. Thus, in the elastic range of the material, the stresses in the structure are directly related to loads imposed on the structure, which in turn are determined by the natural frequencies and mode shapes of the structure, external load environment, and other effects such as shielding, reflections, etc.

4.2 DEPENDENCE OF NATURAL FREQUENCY ON MATERIAL, GEOMETRY, AND SUPPORT

The natural frequency of a structure depends on its material properties, its geometry, the way in which it is supported. For the present study, isotropic material properties such as the modulus of elasticity, Poisson's ratio, and mass density are sufficient. The geometry includes dimensions, wall thickness, and shape. The structure may have various boundary conditions such as free, clamped, pinned, or sliding. For the VETA, the structure is a cantilever beam with one end fixed and one end free. Loading can be in flexure (bending), tension, compression, shear, or torsion. The nature of acoustic loads during the launch of a Space Shuttle may impose bending and probably some torsional loads on the VETA. Lastly, natural frequencies may be associated with extensional deformation, those involving torsional deformation and those caused by flexural deformation. Flexural vibration modes refer to bending deformations normal to the undeformed beam axes. In pure bending deformations, no axial loads are supported by the beam. Flexural or bending modes are of significant importance since their natural frequencies are much lower than those of extensional and torsional modes, and their resulting stresses are consequently greater.

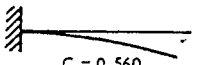
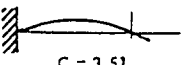

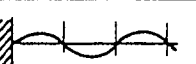
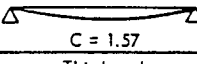
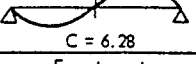
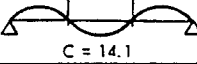
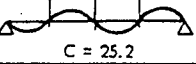
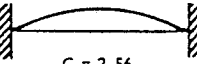
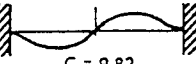

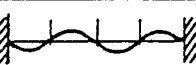
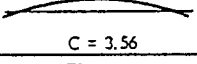
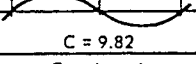
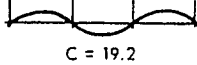
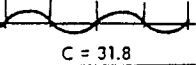
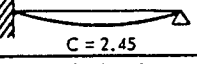
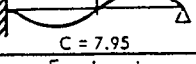
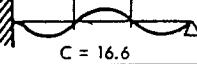
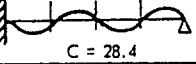
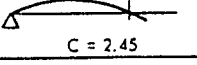
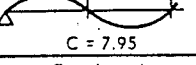
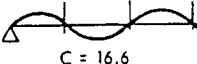
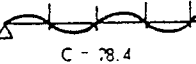
5. FIELD TESTS

5.1 MODAL TESTS

The flexural natural frequencies for many of the structures of interest were analytically computed using closed-form solutions. For a slender cantilever beam, the flexural natural frequency of the beam had the form (see table 2):

$$f_n = C \sqrt{(gEI) / (wL^4)} \quad (1)$$

Table 2. Vibration in Flexure

CANTI-LEVER	Fundamental mode	Second mode
	 $C = 0.560$	 $C = 3.51$
	Third mode	Fourth mode
	 $C = 9.82$	 $C = 19.2$
SIMPLY SUPPORTED ENDS	Fundamental mode	Second mode
	 $C = 1.57$	 $C = 6.28$
	Third mode	Fourth mode
	 $C = 14.1$	 $C = 25.2$
FIXED ENDS	Fundamental mode	Second mode
	 $C = 3.56$	 $C = 9.82$
	Third mode	Fourth mode
	 $C = 19.2$	 $C = 31.8$
FREE ENDS	Fundamental mode	Second mode
	 $C = 3.56$	 $C = 9.82$
	Third mode	Fourth mode
	 $C = 19.2$	 $C = 31.8$
FIXED-HINGED	Fundamental mode	Second mode
	 $C = 2.45$	 $C = 7.95$
	Third mode	Fourth mode
	 $C = 16.6$	 $C = 28.4$
HINGED-FREE	Fundamental mode	Second mode
	 $C = 2.45$	 $C = 7.95$
	Third mode	Fourth mode
	 $C = 16.6$	 $C = 28.4$

where C is a constant determined by the type of the structure support and mode number, L is the length of the beam, E is the modulus of elasticity, I is the moment of inertia about the neutral axis or a principal axis, w is the weight per unit length of the beam, and g is the gravitational acceleration. Table 2 includes C values for beams.

The first three flexural modes of VETA vibration are included in table 3 for a cantilever beam. Special functions (Krylov functions) were used to predict the natural frequencies, mode shapes, bending, and shear moments. For VETA, analytically computed normalized modal parameters using Krylov functions were incorporated into a software program called C-BEAM (see 6.2).

A modal survey was conducted later using the impact hammer excitation technique to establish the natural frequencies, mode shapes, and damping characteristics. The natural frequencies were then compared with those computed analytically using the C-BEAM software. Results of this comparison are included in table 3.

5.2 DYNAMIC TESTS

The test article was installed at a 330-degree azimuth on top of the PTCR roof and exposed to acoustic loads generated by seven launches. The first two launches from Launch Pad A proved crucial for setting measurement ranges and verifying operational features of the entire DAS. The VETA has been in operation since April 1994. Data was acquired during launches from Launch Pad A (near-field) and Pad B (far-field). The data obtained from these launches was used to verify the deterministic theory and a far-field acoustic prediction model (see table 4).

Field measurements and subsequent observations used in assessing the applicability of an analysis method to the launch acoustic loads and response is presented in section 6.

6. ANALYSIS METHODOLOGY

The characteristic level of the loading environment experienced by the VETA and the associated time intervals together defined the various stages of a launch. Engine ignition sequence, the amount of time required for thrust to build up, and vehicle ascent velocity and trajectory all contributed to defining the launch sequences and their duration. Additionally, environmental variables such as wind speed and direction, temperature, and humidity factors affected overall levels.

Table 3. Comparison of Flexural Natural Frequencies [Theoretical (C-BEAM) Versus Modal and Dynamic Tests]

Bending Mode No.	C-BEAM Frequency (Hz)	Modal Test Frequency (Hz)	Dynamic Test	Modal Test Damping (%)
1	8.902	8.836	8.789	0.45
2	55.787	54.309	53.710	0.17
3	156.207	144.004	146.484	0.17
4	306.104	Not available	Not available	Not available

Table 4. Near-Field Acoustic Database

Sensor Designation and Location	Launch Number				
	STS-68	STS-67	STS-71	STS-69	STS-74
KAVPA004A (Front)	✓	X	✓	✓	✓
KAVPA005A (Back)	✓	✓	X	X	X
KAVPA006A (Front)	✓	✓	X	✓	✓
KAVPA007A (Back)	✓	✓	✓	✓	X
KAVPA008A (Front)	✓	✓	✓	✓	✓
KAVPA009A (Back)	✓	✓	✓	✓	✓

Notes:

- ✓ = usable data
- X = partially usable data
- Launch inclination was 57° for STS-68, 28.45° for STS-67 and STS-69, and 51.6° for STS-71 and STS-74.

Launch environment data such as plume pressures, acoustics, strains in structural members, and vibration were random, nonstationary, and wideband in nature. Data time histories represented long-duration transients where both the mean and standard deviation within a short-time interval also varied with time. The location of the VETA within the launch perimeter, its proximity to the Shuttle, and varying launch trajectory/azimuth yielded meaningful data from T-0 to T+17 seconds of Shuttle launch countdown.

6.1 LOAD CHARACTERIZATION

Details of basic and post-processing of launch data for characterization of launch loads were documented in the references in section 9, items d through i. Methods for characterizing acoustic pressures in terms of sound pressure levels (SPL's) that were developed before the start of the Space Shuttle program were replaced by high-resolution power spectral densities (PSD's). Typical functions such as cross-power spectral densities (CPSD's), normalized CPSD's, coherences (COH's), coupled with newly developed functions such as pressure correlation lengths (PCL's) have become common descriptors characterizing the acoustic field. Also, correlated pressure distributions (CPD's) derived from PCL's provided a graphic illustration of vibroacoustic coupling (influence of the acoustic field and its location on the mode shape of a structure). All transient pressure time histories (see appendix C, figures C-1 through C-6) were used as forcing functions for the computations of structural response in individual modes, leading to response spectra (similar to shock spectra).

To enhance the accuracy of the test-analysis correlation, often it was necessary to characterize acoustic loads both in the vertical and horizontal directions. Since the VETA was tall and slender, sensors were installed in the vertical direction only. As a rule of thumb, PCL's were considered valid if they ranged anywhere from three to seven times the distance between two adjacent sensors. VETA sensors were placed at 3-foot and 6-foot intervals.

6.2 ANALYSIS USING THE C-BEAM PROGRAM

For this project, new software was developed specifically to compute resonance's and modal parameters of a uniform cantilever beam analytically using Krylov functions. The program computed stresses (bending moments and shears) resulting from each normal mode. All modes were normalized to a "unit" maximum modal displacement. Plots of normal mode shapes and internal stresses were output to a printer (see appendix D, figures D-1 through D-4).

However, of significance was the fact that once modal parameters were computed analytically, the program calculated J coefficients (or the square root of the joint

acceptances) required for vibroacoustic analysis. J coefficients were calculated for all positions of the center of a CPD along the cantilever span. This option, however, required actual PCL's computed from dynamic test data, corresponding to each resonance of a normal mode. Both the average J value and the maximum or peak J value were output. For design purposes, values of the peak J values and the location of the CPD center along the span were necessary. Knowledge of VETA characteristics using the C-BEAM program provided valuable insight into the bounds of various parameters used for test-analysis correlation.

6.3 RESPONSE CHARACTERIZATION

Earlier KSC documentation (see references in section 9, d through i) presents computations of the "peak" dynamic response of a normal vibration mode of a structure to an input transient. The deterministic method was based on the knowledge of modal parameters (natural frequency, mode shape, and damping from a modal test), response spectra to acoustic pressures (response spectra plots), and a definition of the acoustic field by means of PCL's. A PCL was a way of defining the distribution pressure field along the length of the beam and required the knowledge of COH and phase (PHA) between two sensors or points on the structure. PCL's significantly longer than the length of the structure implied a uniformly distributed pressure field. Correlated pressure distributions were in turn derived from PCL's.

The time history of acoustic pressures, $p(t)$, was assumed to be known from the measurements taken in the acoustic field where the structure was located. Response spectra computations were then made for all available multiple launch/sensor data combinations (see table 3). Generally, a multitude of measurements was required for a proper definition of all basic parameters in an acoustic field that is highly uncorrelated or nonuniform.

The deterministic analysis facilitated the computation of a generalized modal load defined by $G(t)$, where $G(t) = AJ * p(t)$. AJ defined the vibroacoustic coupling between the structural response and the acoustic field. AJ was computed using previously obtained CPD's and modal displacements or individual mode shapes of the structure.

Response spectra and PCL's were assumed available for the frequency containing at least the first four normal modes. The calculation of generalized modal loads was then reduced to the problem of estimating AJ coefficients for each normal mode and peak response modal coordinates, which were computed from response spectra. Utilization of response spectra, $Y = q * \omega_1^2 / (AJM)$, to acoustic pressures, $p(t)$, was in the application to the analysis of peak structural responses.

Generalized modal loads were defined by means of AJ coefficients. AJ coefficients were a measure of the vibroacoustic coupling between the acoustic field and the structure; the stronger the coupling was, the higher the vibration of the structure in a coupled mode was. Thus, an accurate estimate of AJ values for each vibration mode was essential to the calculation of dynamic response. However, even for a structure of average complexity, computing AJ values were often cumbersome because existing dynamic analysis codes did not account for all parameters leading to extreme AJ's. AJ's depended on the surface integral of the product between the modal displacements and the correlated pressure distribution (a function of the pressure correlation lengths), which in turn depended on the type of acoustic field and resonance mode of that structure. Lastly, the relative position between the mode and the center of the pressure distribution also affected the variable integral limits and affected the AJ values. Generally, a different position of the correlated pressure distribution corresponded to each vibration mode, resulting in the strongest vibroacoustic coupling and highest structural response.

While many vibration modes were excited in a wide-band acoustic field, stress-strain extremes governing a design occurred mainly in a single fundamental mode of each and every structural component. Typically, the first three normal modes should be considered for design, assuming that the structure responds to them. For most launch pad structures in the near-field that were exposed to the acoustic field during the first 17 seconds after liftoff, the number of acoustic load cycles were not significant enough to induce full resonance at higher than the fundamental mode. For all practical purposes, the GSE structures were governed by the first mode for design purposes. Strain and vibration response time histories are included in appendix E, figures E-1 through E-7.

7. ANALYSIS-TEST CORRELATION

A significant effort was made to process and generate statistics based on multiple launches to enhance prediction accuracy and confidence limits. However, sensor failures coupled with varying launch trajectories and environmental factors restricted the availability of launch data for this study (see table 4). Since this was the first attempt at validating the deterministic model, it was decided to limit the variability of the acoustic load and subsequent strain response by using available launch statistics. Despite these shortcomings, the VETA project provided valuable insights into the understanding of the characteristics of launch-induced acoustic loads and how these dynamic loads must be considered in launch environment design criteria.

7.1 CORRELATION PROCEDURE

Processed data from Shuttle launches were carefully reviewed to establish whether or not the VETA was exposed to adequate acoustic loads. Adequacy of strain response was verified by comparing the data to prior analytical work.

Test correlation provided dual advantages: (1) established the validity or applicability of the deterministic method of analysis for predicting the response of structures especially in the low frequencies and (2) allowed the development and use of a simplified concept called the equivalent static load. The concept of equivalent load provided a means for the designers of ground system facilities and equipment to account for launch-induced acoustic loads without resorting to cumbersome and sophisticated dynamic analysis methods at least in the preliminary stages of the design process. Test-analysis correlation consisted of the following:

- a. Identification of structural resonances using tip accelerometer and strain gage measurements.
- b. Computation of the net effective load on the VETA using front and back pressures
- c. Calculation of the response spectra values using the net effective load (Y values)
- d. Computation of PCL values using PSD's, CPSD's, and COH functions
- e. Evaluation of maximum or peak value of joint acceptances (J's) for first vibration mode and unique load location
- f. Computation of predicted strains from knowledge of the bending moment at the section where the strain gage is located
- g. Comparison of predicted strains using the deterministic method with those measured on the VETA at a specific location
- h. Validation of the deterministic method

7.2 GENERAL OBSERVATIONS

The following key findings were made during the analysis test program:

- a. The acoustic load environment experienced by the VETA was indicative of a uniformly distributed load with no significant phase shifts.
- b. Launch-to-launch variability of acoustic load data was dictated by launch inclination. Higher inclinations (51 to 57 degrees) resulted in higher loads.
- c. The VETA was subjected primarily to flexural vibration. The torsional load on the structure was insignificant.
- d. Higher acoustic loads were observed on the VETA front face during liftoff (T-0 to T+7 seconds), with lower loads being observed during the Shuttle roll maneuver (T-10 to T+17 seconds). Acoustic loads on the back face of the VETA indicated the opposite, with loads during the roll maneuver being almost twice those observed on the front.
- e. The orientation of the VETA along the plume direction (vertical) also affected correlation. Typically, horizontal structures yielded longer PCL's than those oriented vertically.
- f. PCL computations were found acceptable below 20 hertz. PCL's that were based on sensors placed at 3- and 6-foot distances were used in the analysis.
- g. The actual load-carrying capacity of the VETA is higher than the design. This is due to the cancellation of the front and back pressures.
- h. Test data limitations restricted comparison of data from different launches. For this project, the STS-68 launch was used.
- i. Only the first fundamental frequency was significantly excited. Test, analysis, and modal models were in reasonable agreement with the C-BEAM program.
- j. No significant modal coupling was observed during the modal test. The first four natural frequencies observed were all well separated and distinct.

7.3 CORRELATION RESULTS

The test-analysis correlation effort focused primarily on the application of processed data in establishing how well the analytically predicted strains compared with those measured on the VETA for a specific location. A significant effort was expended in understanding the nature of acoustic excitation and its effect on the strain response, tip accelerations, and displacements. Cross-functions were also computed between acoustics/acceleration, acoustics/strains, strains/accelerations, and front and back pressures. For brevity, only important findings are documented in this report. All conclusions were derived from observations of test and analytical data, which are extensive and, therefore, not presented here.

Net effective pressures rather than front-only or back-only pressures yielded the most accurate correlation. In the past, only the front face of the structure was instrumented. This resulted in a response 20 to 30 percent lower than when front-back pressures were considered. This indicated that some structures can carry a higher net effective load and still not fail. The slenderness, orientation, location on the launch pad, and whether or not full resonance was induced all play a key role in the failure of pad structures. Use of response spectra values based on 95-percent prediction limits overestimated the measured response in the near-field by about 10 percent. For complex studies such as random vibration and with the limited availability of data, this variation seemed reasonable. It should be noted that this validation was made for the first mode only. The effect on higher modes needs to be studied.

A new zone was identified in the near-field, 100 feet beyond the vehicle centerline and about 300 feet within the vehicle centerline. This was called the plume impingement zone or plume affected zone. For all future designs, this effect must be considered, since the acoustic loads can be at least 100 percent higher than those observed during peak liftoff.

Appendix F summarizes the test-analysis correlation effort with the use of actual computations for the VETA for the first mode only, since the first mode was excited. The computations document the results for a 6-foot sensor distance. However, sufficient data was available to compute a similar verification for 3-foot sensor distances.

8. CONCLUSIONS

The launch environment database (used to verify the deterministic approach), though small, proved valuable in understanding the dynamic loads experienced by various launch pad structures in the near-field. While characterizing the acoustic loads is important, their consideration in the design of launch pad structures is of

greater consequence. Based on the present effort, it can be concluded that the concept of an equivalent load and the deterministic method of analysis on which it is based is suitable during the preliminary design process. For critical structures a more exhaustive and detailed analysis is in order.

Many architectural and engineering firms are familiar with the concept of equivalent load when confronted with dynamic loads (wind, earthquake, pressure, aerodynamic, water waves etc.). Using this technique, inhouse designers can develop a large knowledge base for the modification of existing structures and design of new structures.

Past GSE design was solely based on the liftoff peak acoustic loads. Depending on the type of structure, launch pad location, and exposure to the launch environment, the assessment of the net effective loads and plume impingement effects must also be included in the design process.

Additional launch measurements are highly recommended. This will significantly enhance the database for further validation of the deterministic method and for analyzing the influence of external parameters on the predicted response.

9. BIBLIOGRAPHY

- a. Sonic and Vibration Environment for Ground Facilities - A Design Manual, prepared for NASA-MSFC by Wyle Laboratories under contract NASA-11217, March 1968
- b. Lin, Y.K., Probabilistic Theory of Structural Dynamics, Robert Kreiger Publishing Company, 1976
- c. Bendat, J.S., and Piersol, A.G., Random Data: Analysis and Measurement Procedures, John Wiley & Sons, Inc., 1986
- d. KSC-DM-3147, Procedure and Criteria for Conducting a Dynamic Analysis of the Orbiter Weather Protection System on LC-39B Fixed Service Structure September 1987
- e. KSC-DM-3265, Computation of Generalized Modal Loads in an Acoustic Field Defined by a Distribution of Correlated Pressures, August 1989
- f. GP-1059, Volume III, Environment and Test Specification Levels Ground Support Equipment for Space Shuttle System Launch Complex 39, November 1991

- g. KSC-DM-3613, Structural Response to Launch-induced Nonstationary Random Acoustic Excitation, September 1992
- h. KSC-DM-3649, Liftoff Response Spectra to Space Shuttle Launch-Induced Acoustic Pressures, April 1993.
- i. A Verification of the Deterministic Method to Predict Structural Response to Shuttle Launch-induced Nonstationary Random Acoustic Field; a technical note to NASA/KSC, December 1993.
- j. C-BEAM Program: internal NASA KSC unpublished documentation, April 1994.

APPENDIX A
VETA DESIGN DETAILS

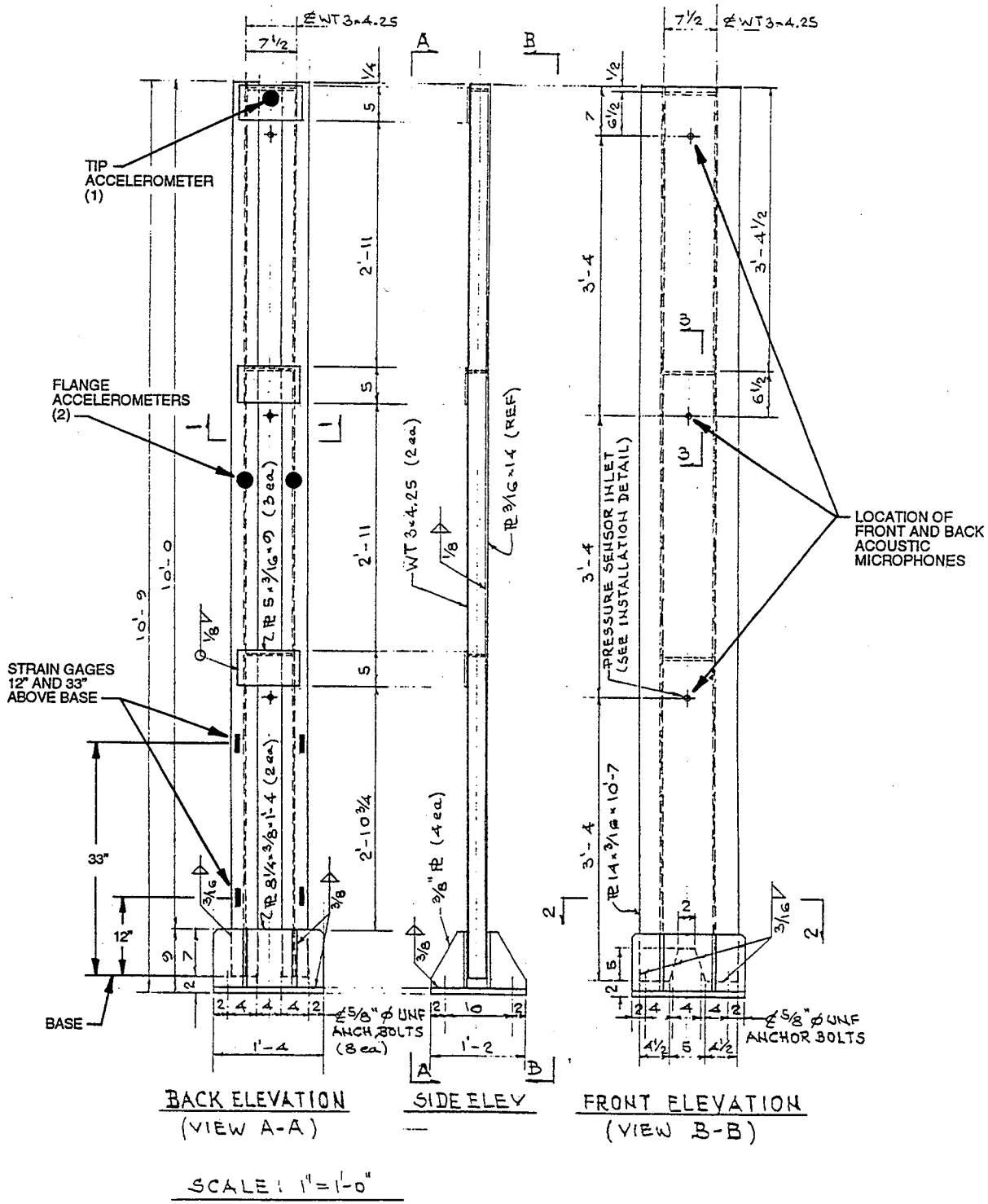


Figure A-1. Test Article (Elevations)

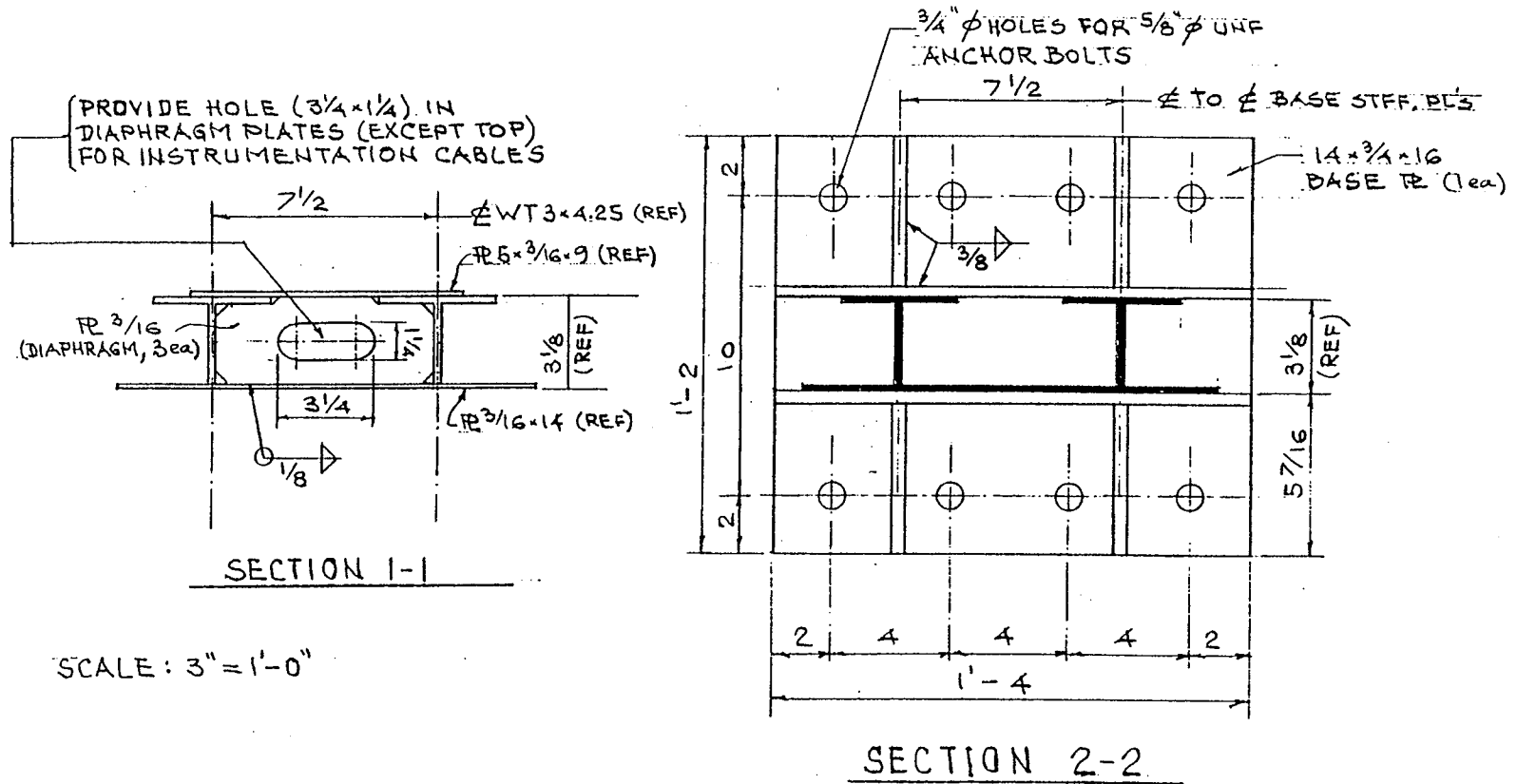
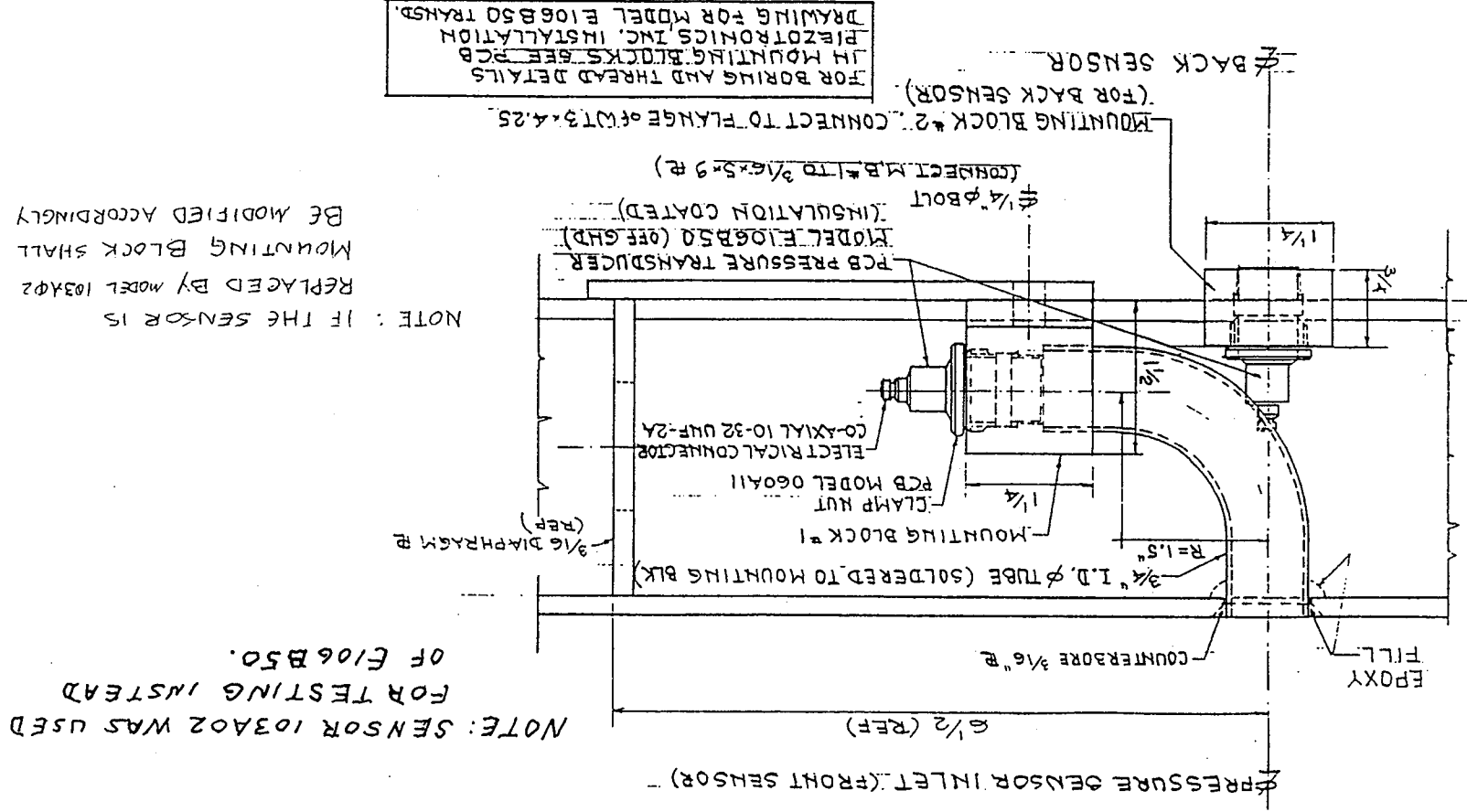


Figure A-2. VETA Drawings (Plan)



FOR BORING AND THREAD DETAILS
 IN MOUNTING BLOCKS SEE PCB
 PIEZOTRONICS INC. INSTALLATION
 DRAWING FOR MODEL E106B50 TRKSD.

Figure A-3. Pressure Sensor Installation Details
 (Scale 1:1)

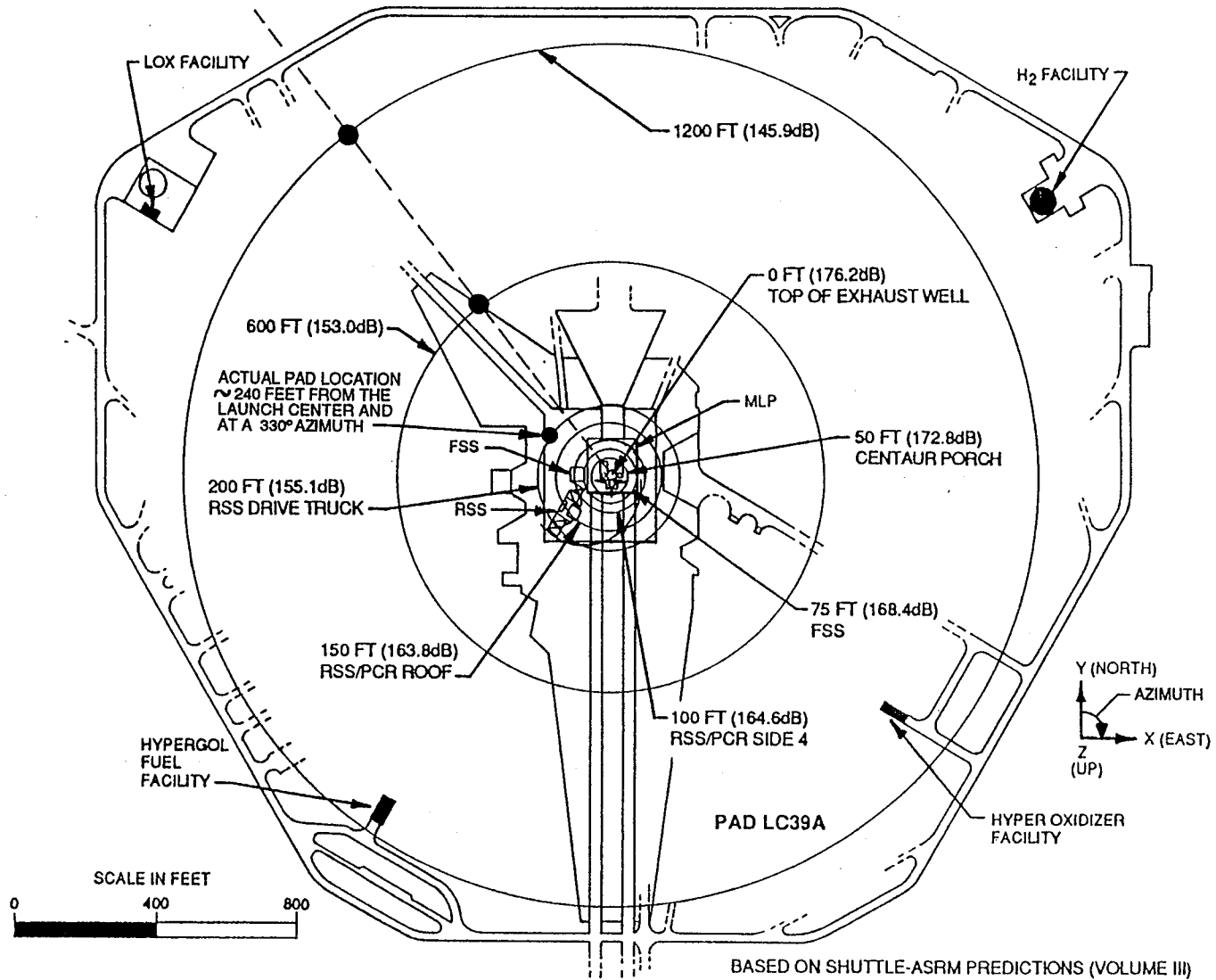


Figure A-4. Test Article Launch Pad Location

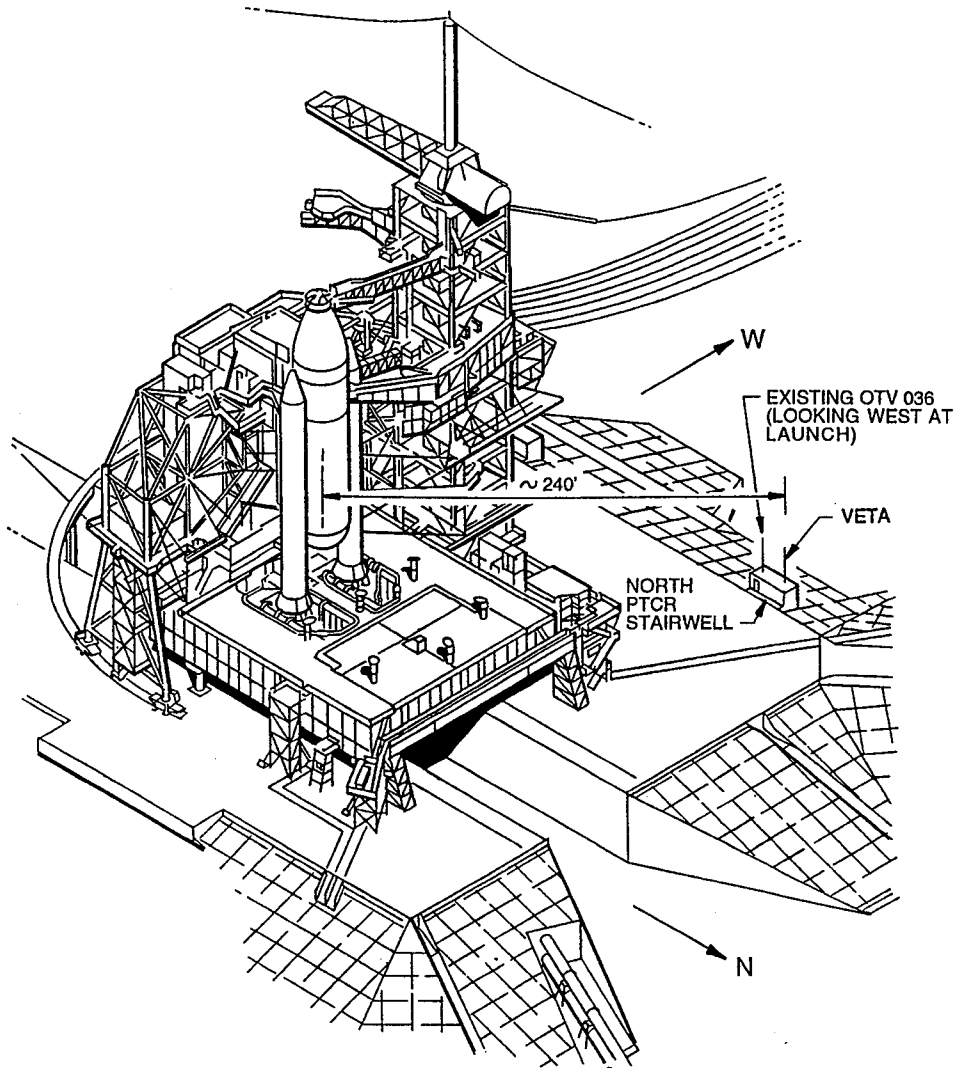


Figure A-5. VETA Location on Launch Pad 39A

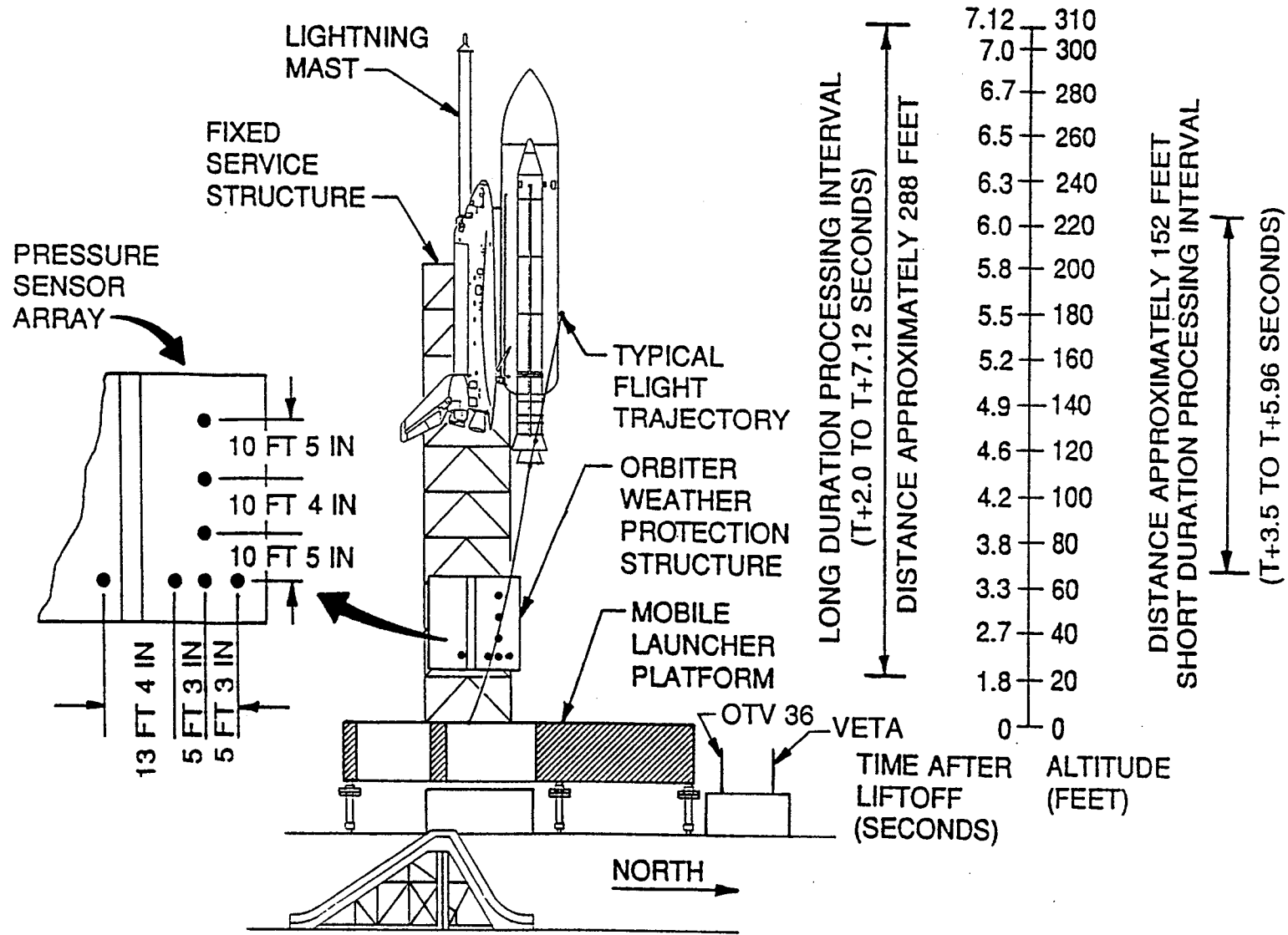


Figure A-6. Shuttle Launch Showing Launch Trajectory

APPENDIX B
DATA ACQUISITION SYSTEM

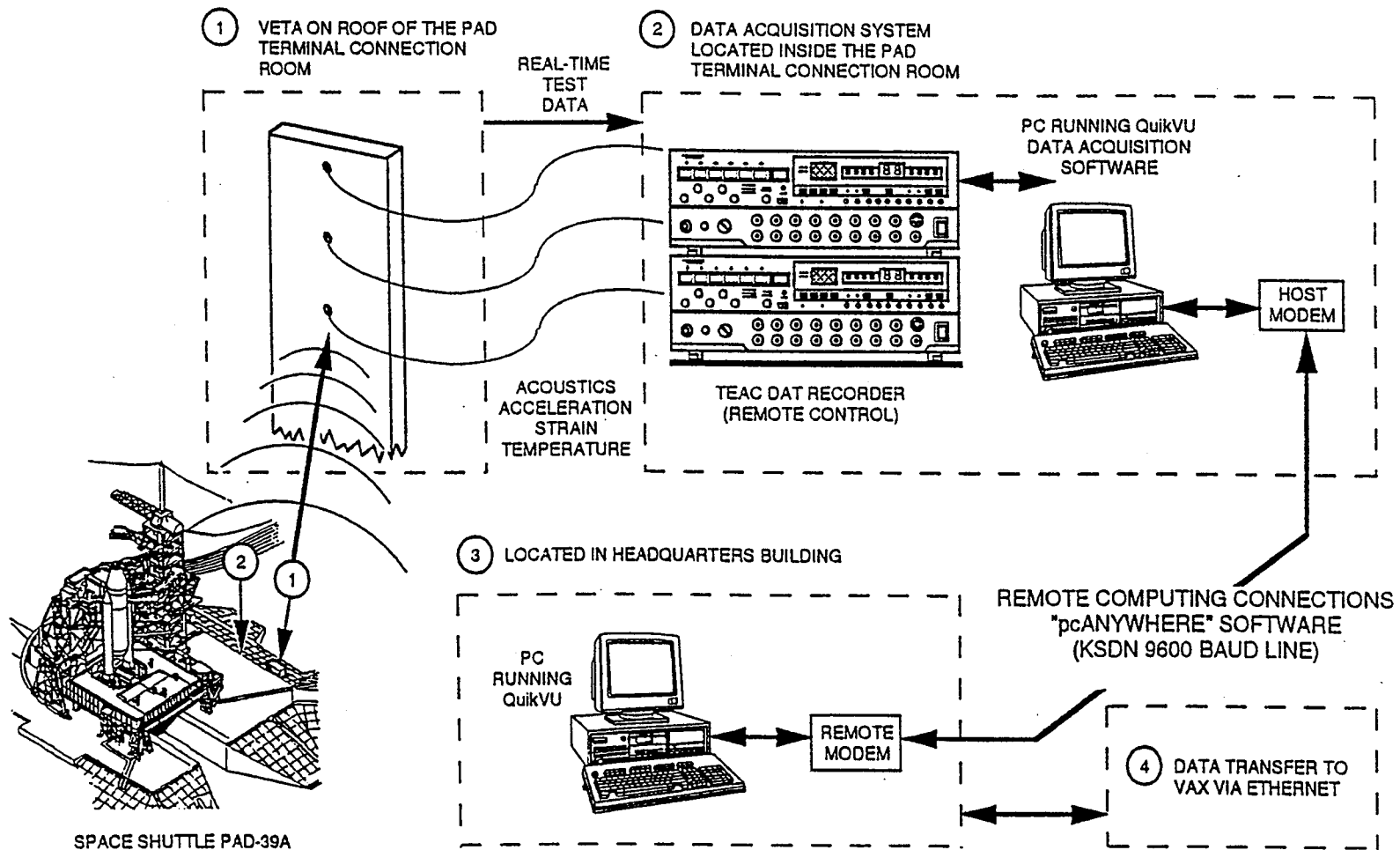


Figure B-1. VETA DAS Subsystems

APPENDIX C
ACOUSTIC LOAD DEFINITION

STS-68 LAUNCH S-0007 09/30/94

Parallel Function Time History Plot

VEITA REPORT - 0011
I)KAVPA004A - VEITA, FRONT, 113 ABOVE BASE FACING EAST
Counts
-2.000 - 2.000 PSIG
Min: -1.290 Time: 11:16:09.501 Max: 1.039 Time: 11:16:09.345 01

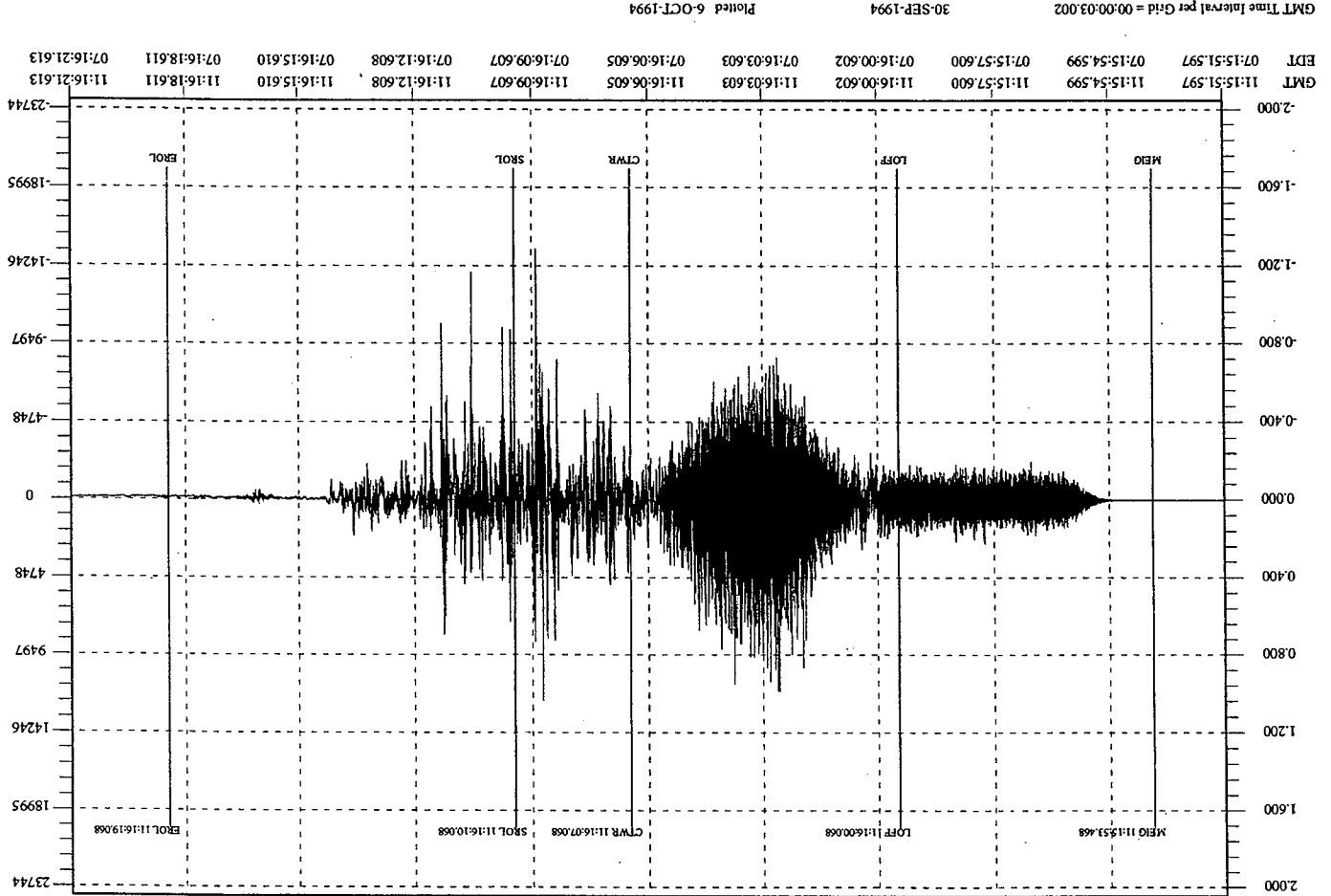


Figure C-1. Pressure Time History (KAVPA004A) - VEITA, Front, 113 Inches Above Base Facing East

GMT Time Interval per Grid = 00:00:03.002
30-SEP-1994
Printed 6-OCT-1994

VETA REPORT - 0012
KAVPA005A - VETA, REAR, 113 ABOVE BASE FACING WEST
Parallel Function Time History Plot
Min: -1.159 Time: 11:16:10.180 Max: 1.456 Time: 11:16:11.004 01 Counts

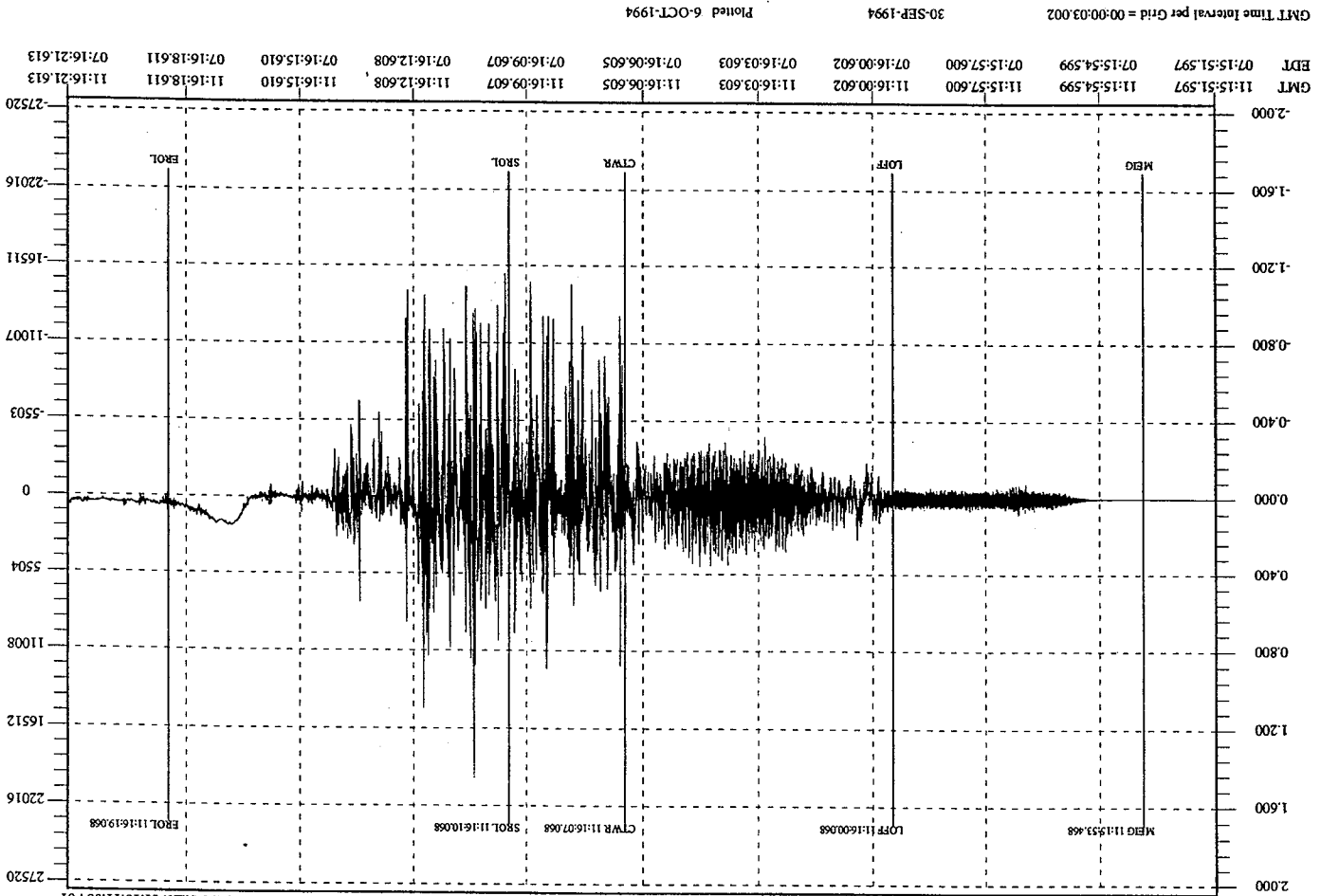
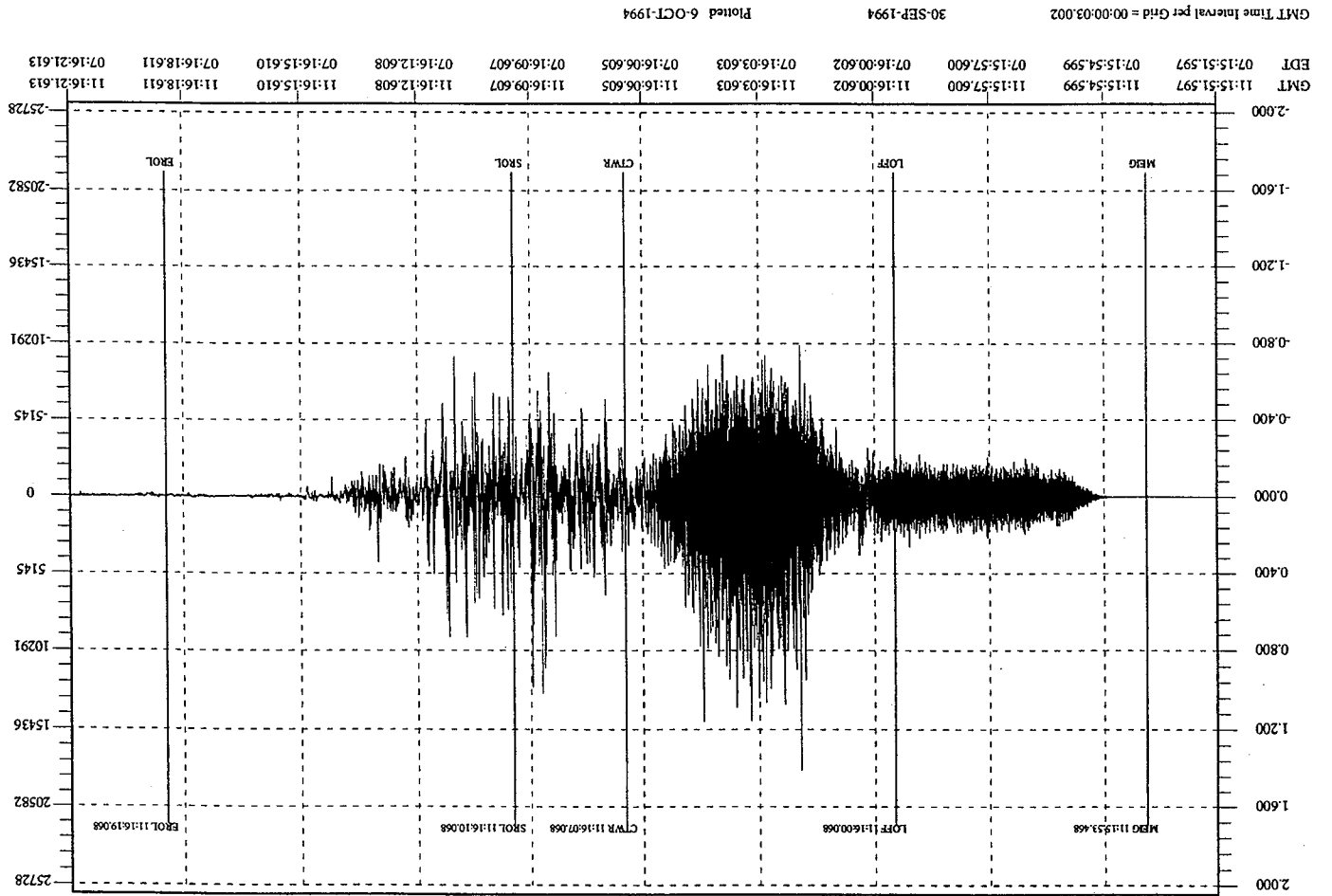


Figure C-2. Pressure Time History (KAVPA005A) - VETA,
Front, 113 Inches Above Base Facing West

STS-68 LAUNCH S-0007 09/30/94
Parallel Function Time History Plot

VETA REPORT - 0013
1)KAVPA006A - VETA, FRONT, 73 ABOVE BASE FACING EAST
Counts
-2.000 - 2.000 PSIG
Min: -0.788 Time: 11:16:02.557 Max: 1.410 Time: 11:16:02.555 01



GMT Time Interval per Grid = 00:00:03.002
30-SEP-1994
Plotted 6-OCT-1994

Figure C-3. Pressure Time History (KAVPA006A) - VETA,
Front, 73 Inches Above Base Facing East

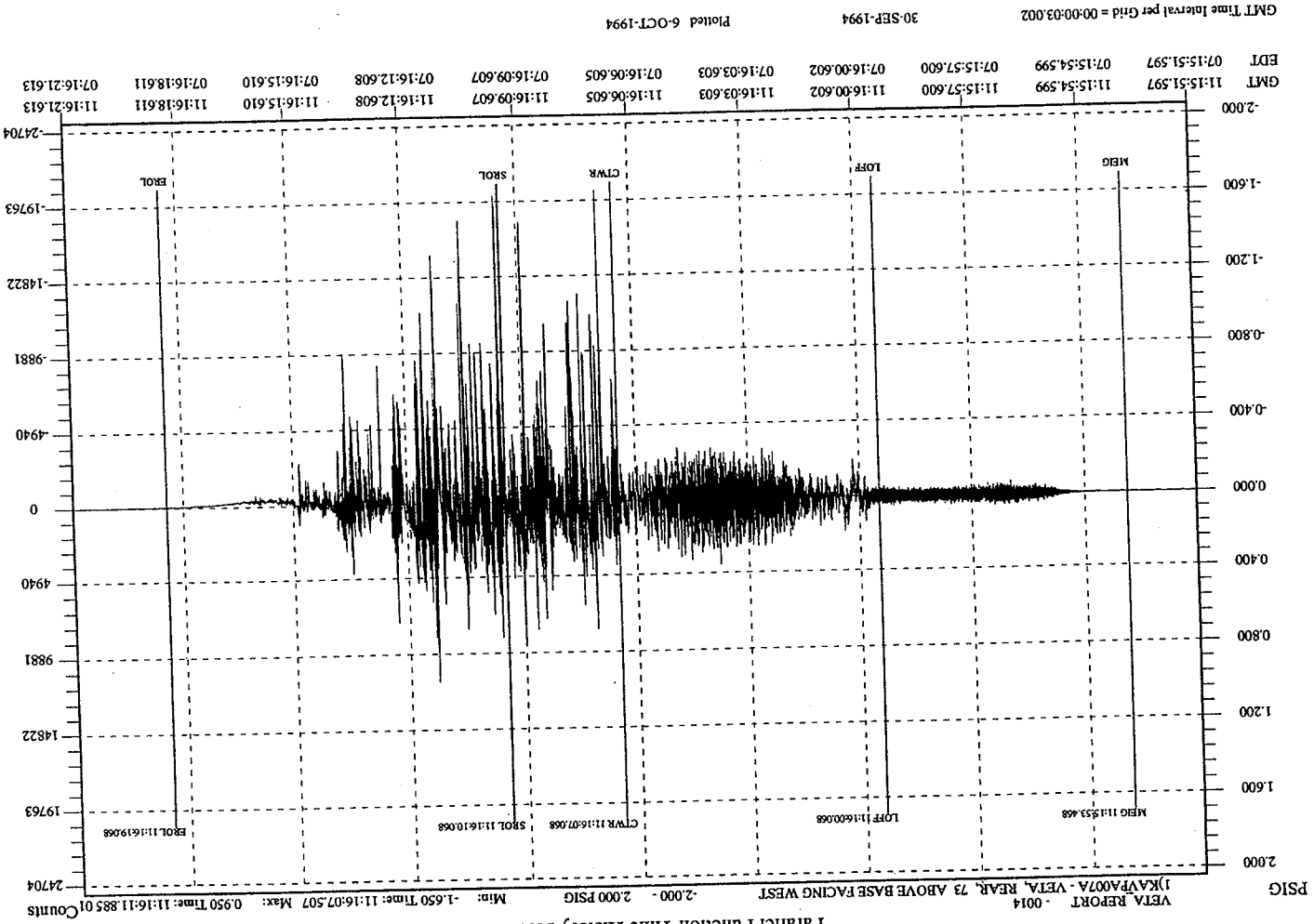


Figure C-4. Pressure Time History (KAVPA007A) - VETA, Rear, 73 Inches Above Base Facing West

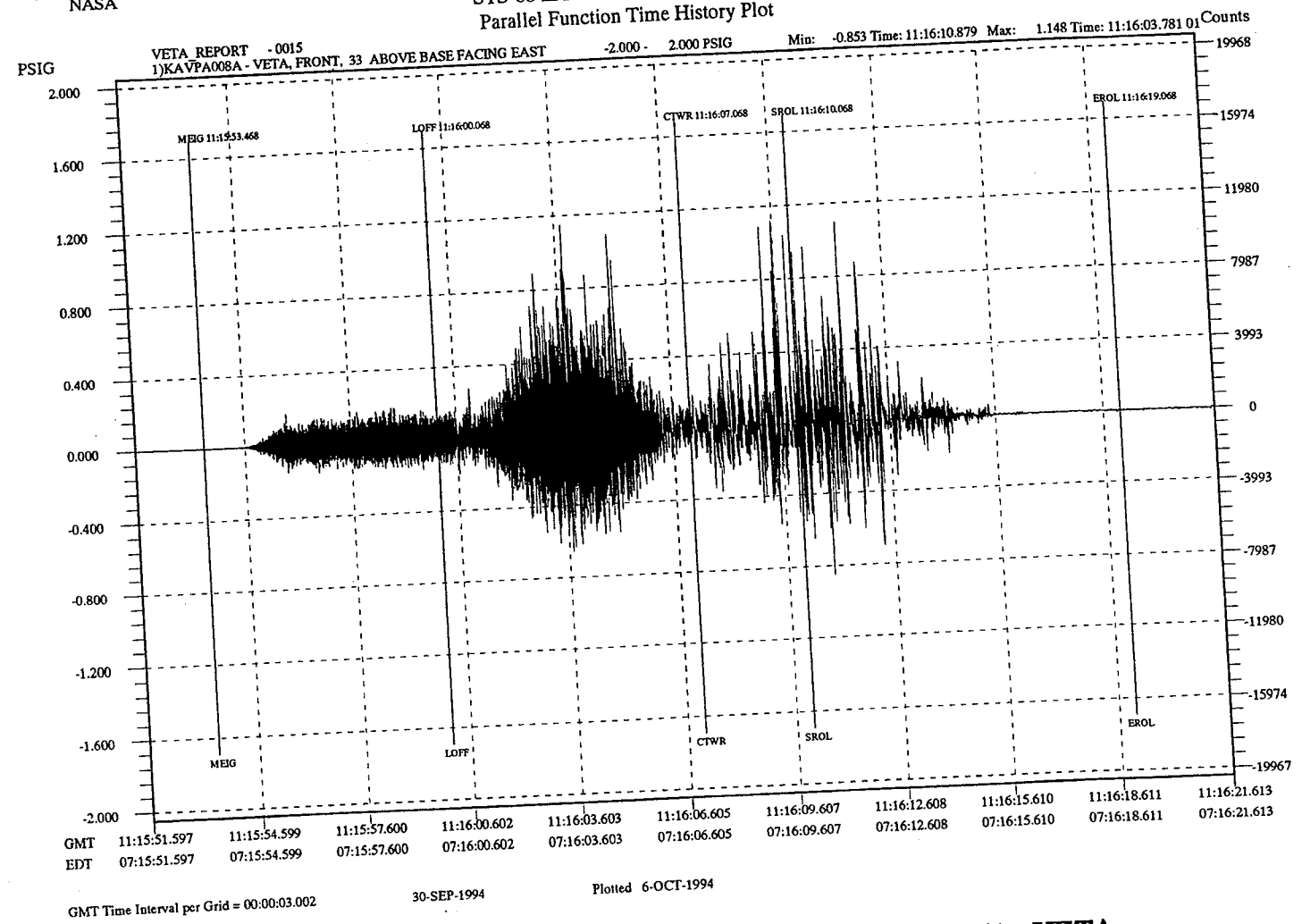


Figure C-5. Pressure Time History (KAVPA008A) - VETA,
Front, 33 Inches Above Base Facing East

STS-68 LAUNCH S-0007 09/30/94
Parallel Function Time History Plot

VEVA REPORT - 0016
KAVPA009A - VETA, REAR, 33 ABOVE BASE FACING WEST
Counts
Min: -1.396 Time: 11:16:11.840 Max: 1.506 Time: 11:16:11.869 01

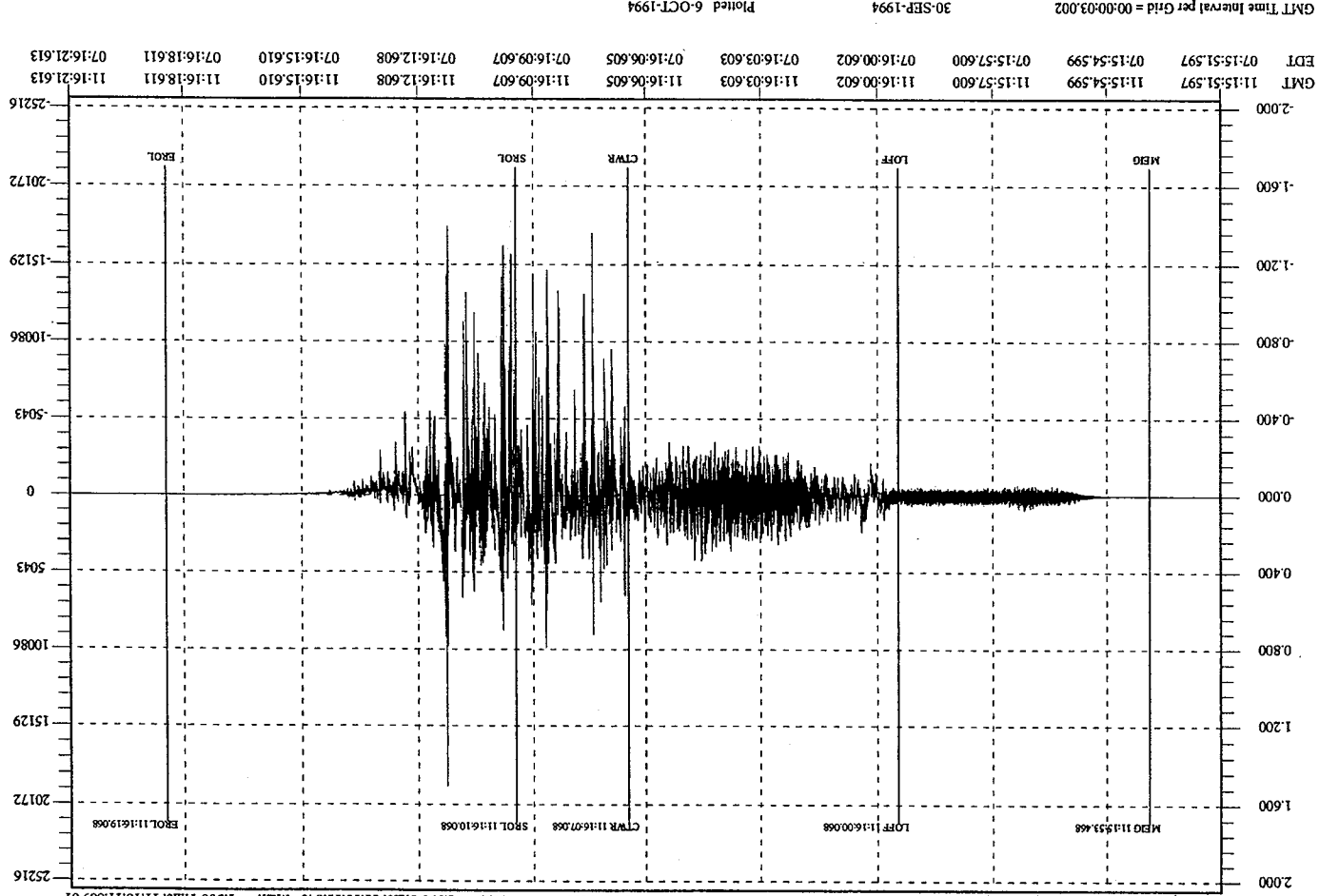


Figure C-6. Pressure Time History (KAVPA009A) - VETA, Rear, 33 inches Above Base Facing West

GMT Time Interval per Grid = 00:00:03.002
30-SEP-1994
Plotted 6-OCT-1994

APPENDIX D

C-BEAM PROGRAM OUTPUT

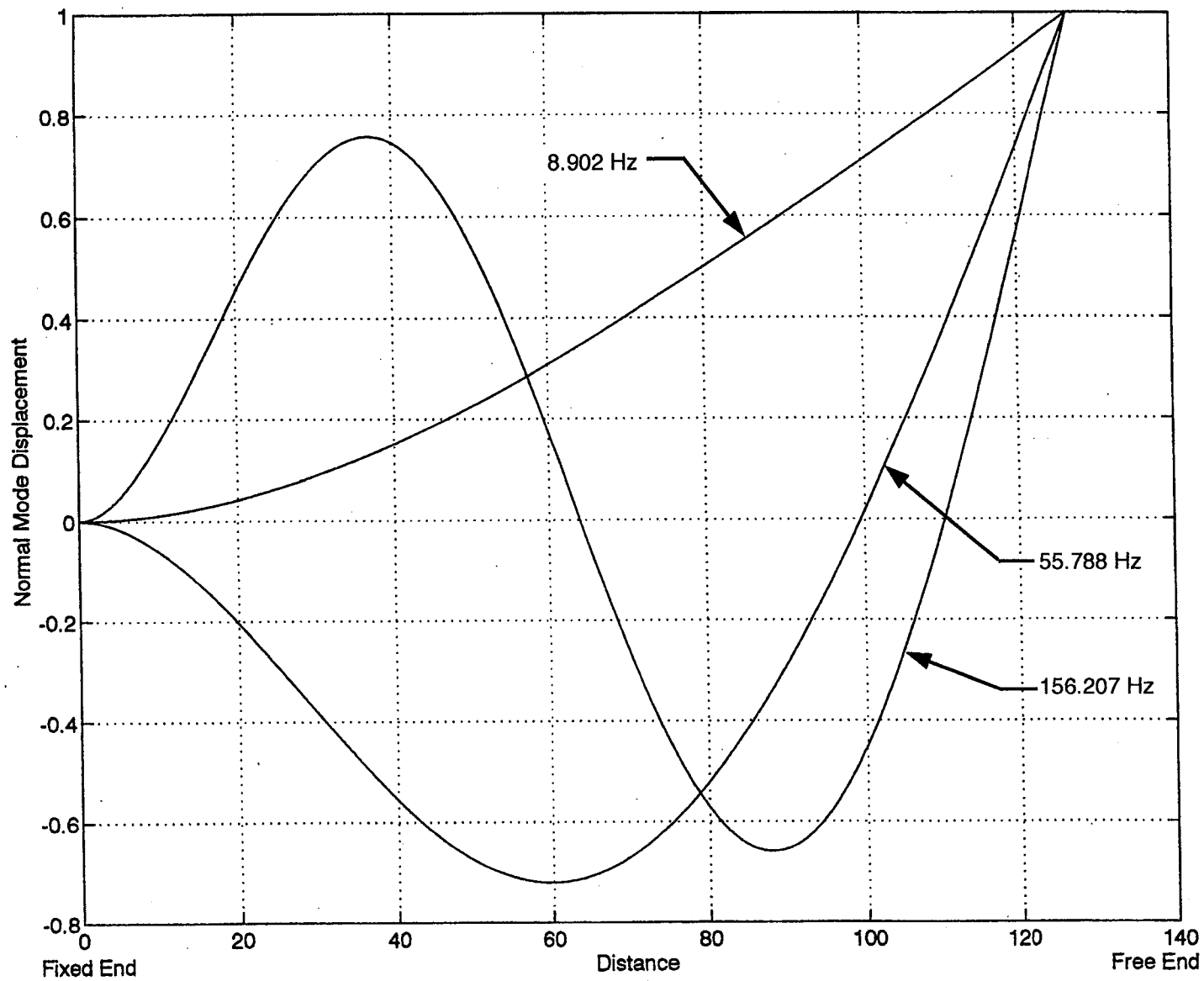


Figure D-1. Cantilever Bending Modes; Resonance Frequency = 8.902 Hz, 55.788 Hz, and 156.207 Hz

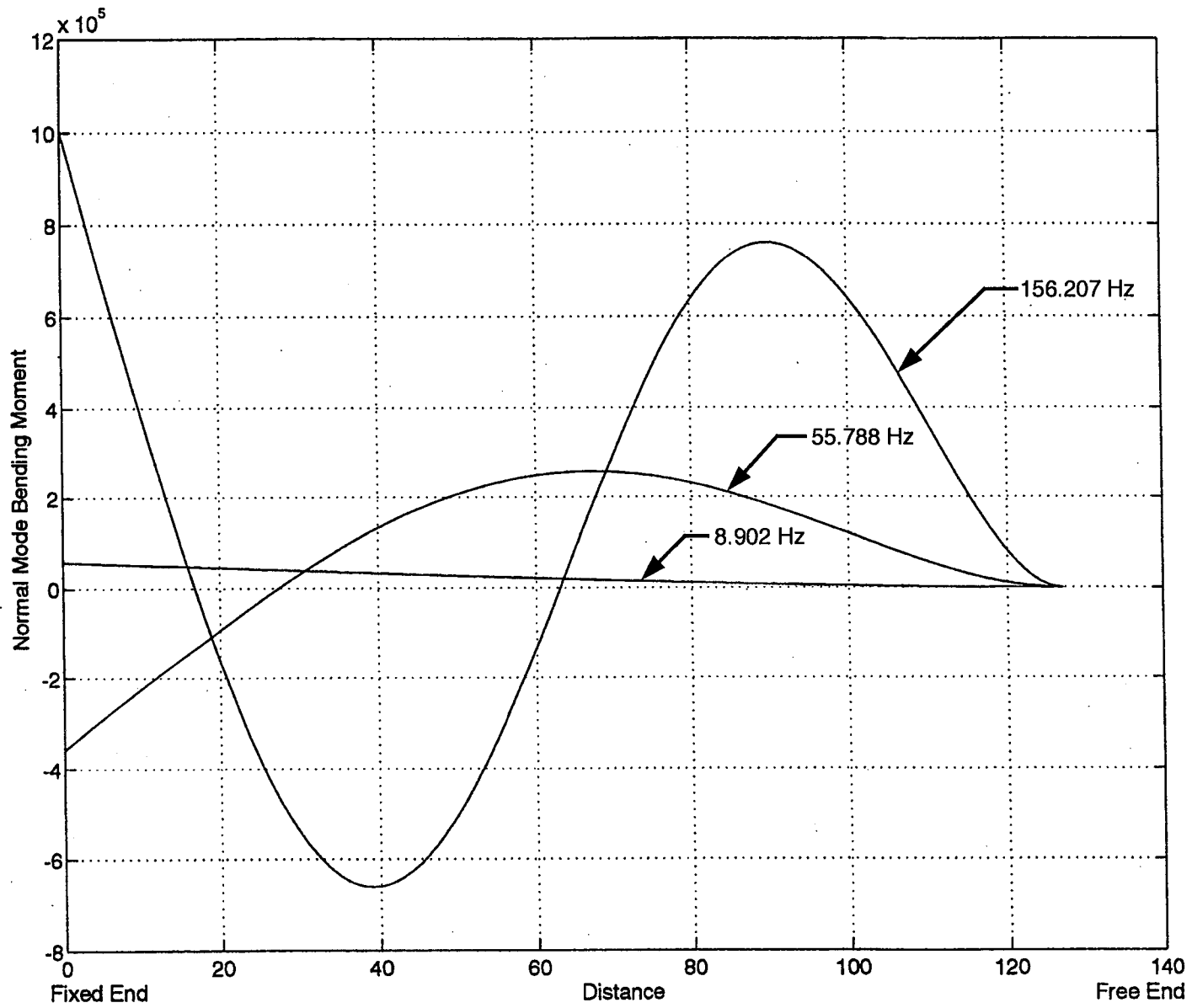


Figure D-2. Cantilever Bending Modes; Resonance Frequency = 8.902 Hz, 55.788 Hz, and 156.207 Hz

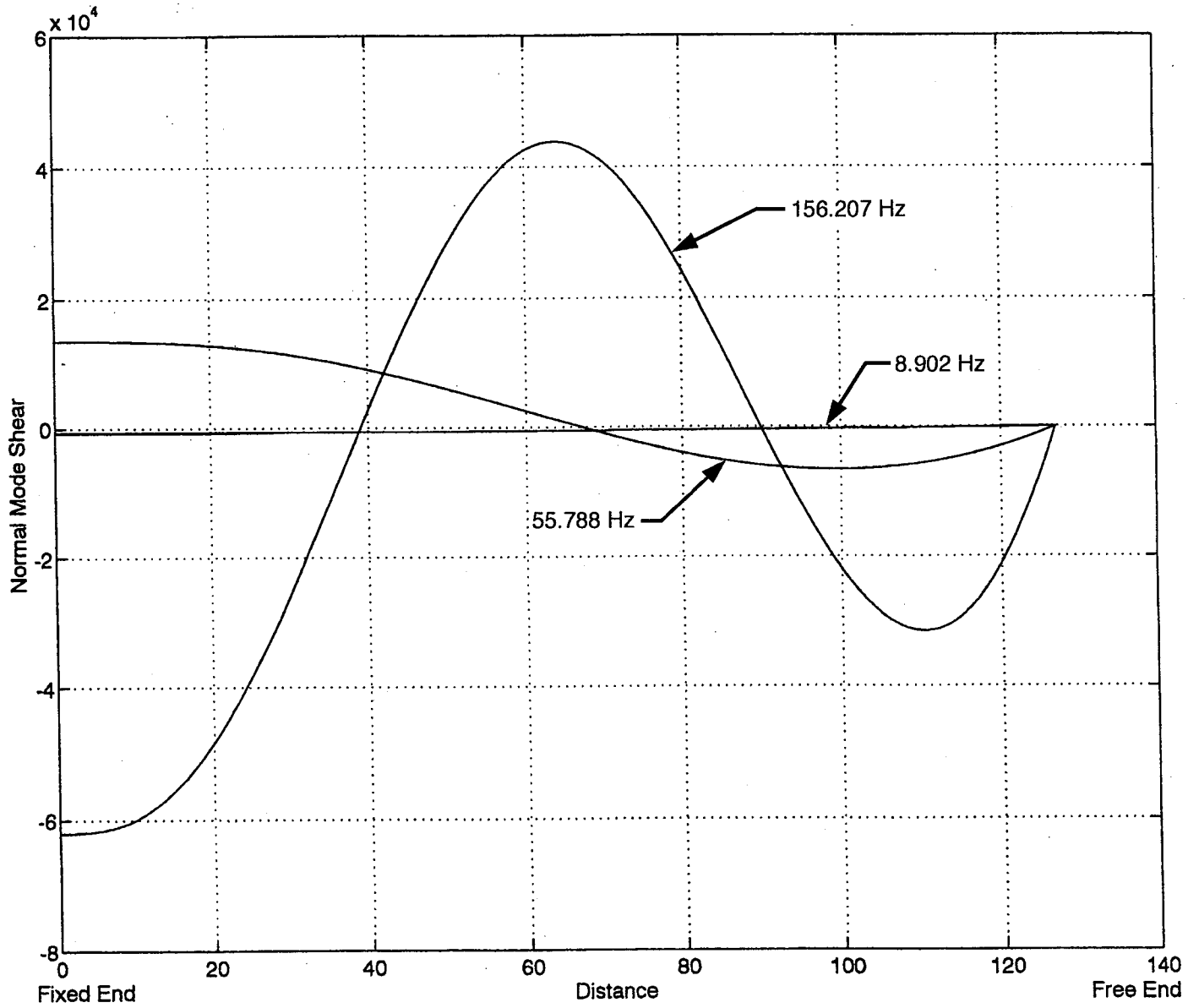


Figure D-3. Cantilever Bending Modes; Resonance Frequency = 8.902 Hz, 55.788 Hz, and 156.207 Hz

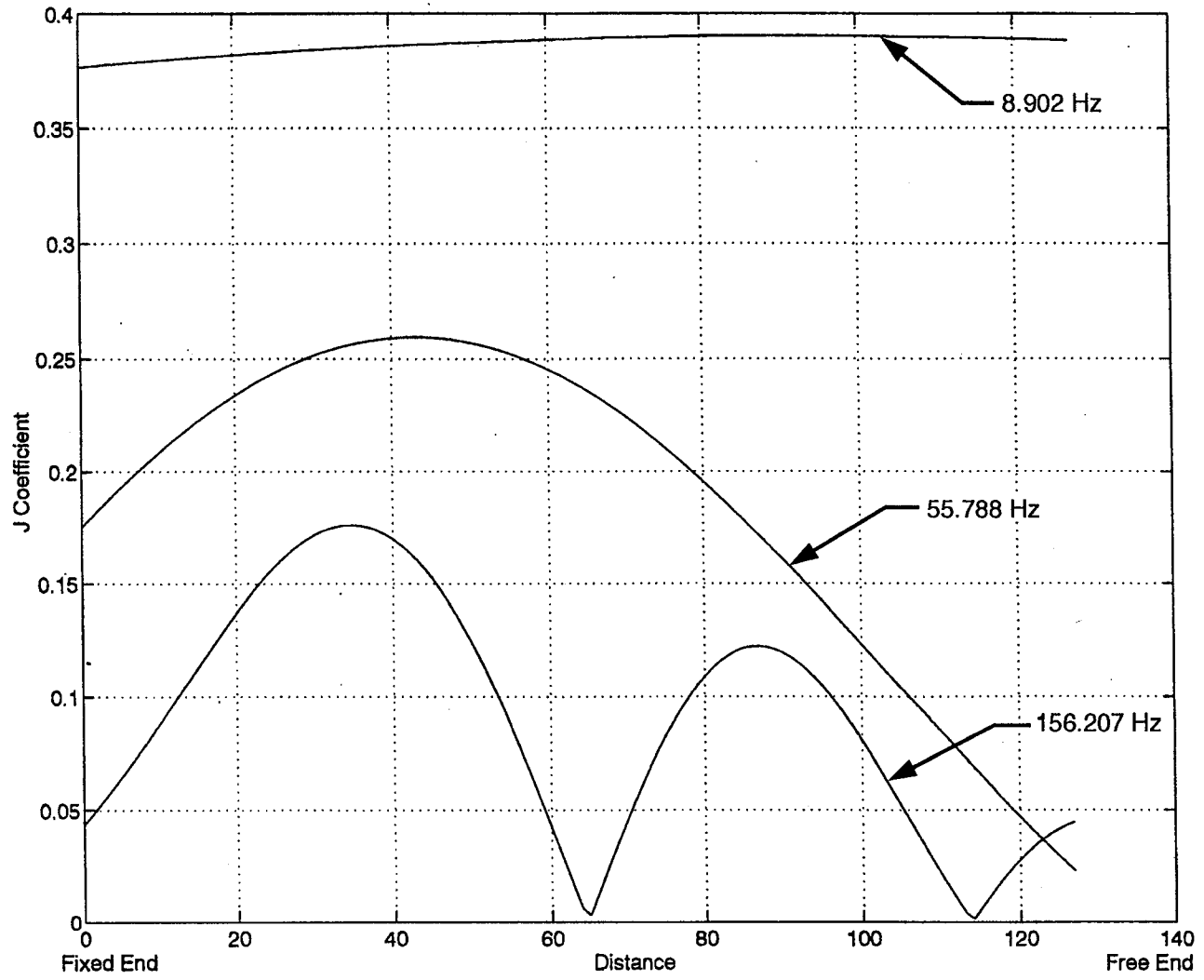


Figure D-4. Cantilever J Coefficient Modes; Resonance Frequency = 8.902 Hz, 55.788 Hz, and 156.207 Hz

APPENDIX E
STRUCTURAL RESPONSE

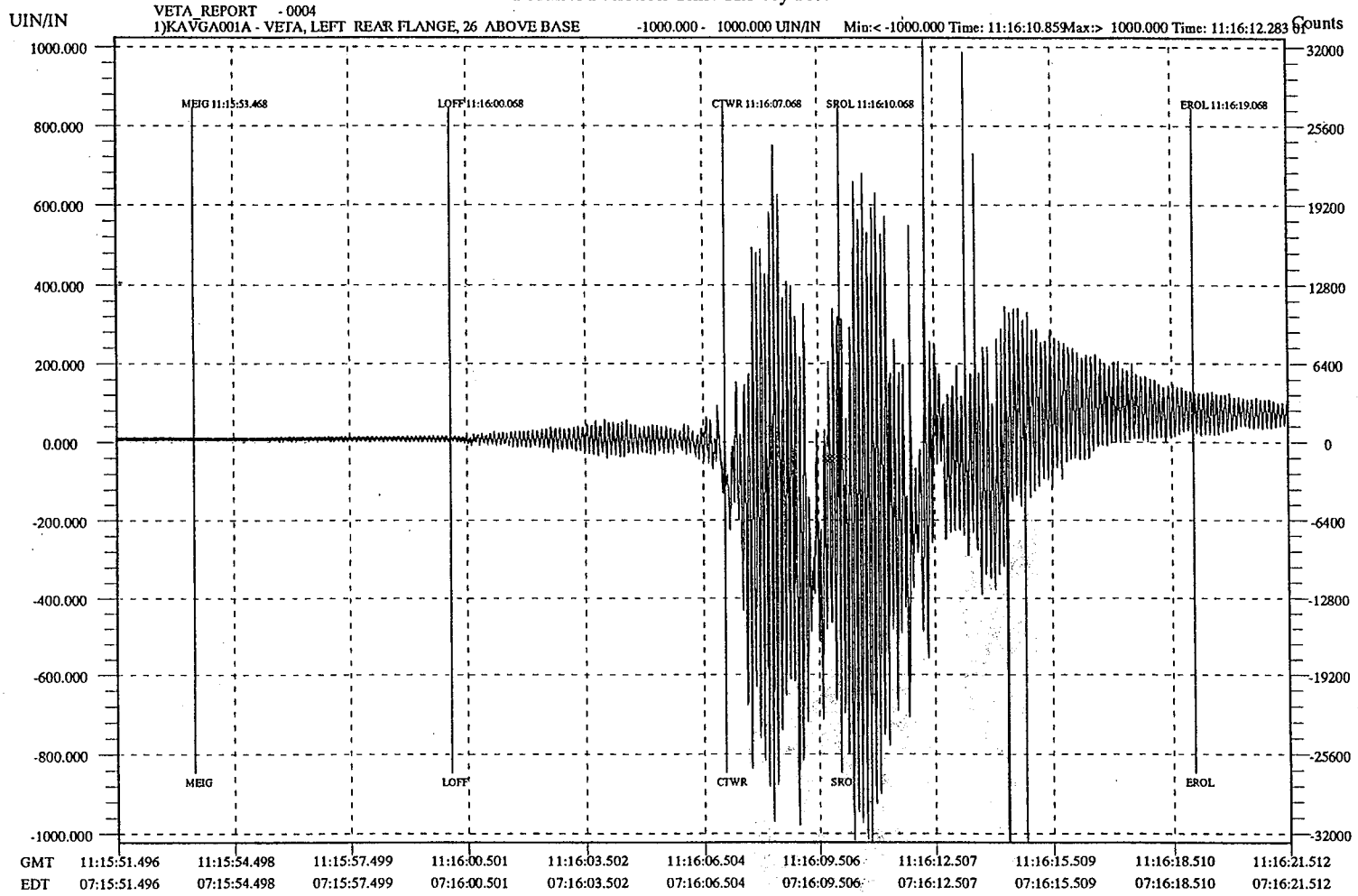


Figure E-1. Strain Response (KAVGA001A) - VETA, Left Rear Flange, 26 Inches Above Base

DATA PROCESSING SYSTEM
STS-68 LAUNCH S-0007 09/30/94
Parallel Function Time History Plot

VETA REPORT -0005
1)KAVGA002A - VETA, RIGHT REAR FLANGE, 26 ABOVE BASE
Counts
Min: < -1000.000 Time: 11:16:10.743 Max: 790.875 Time: 11:16:08.373 Of

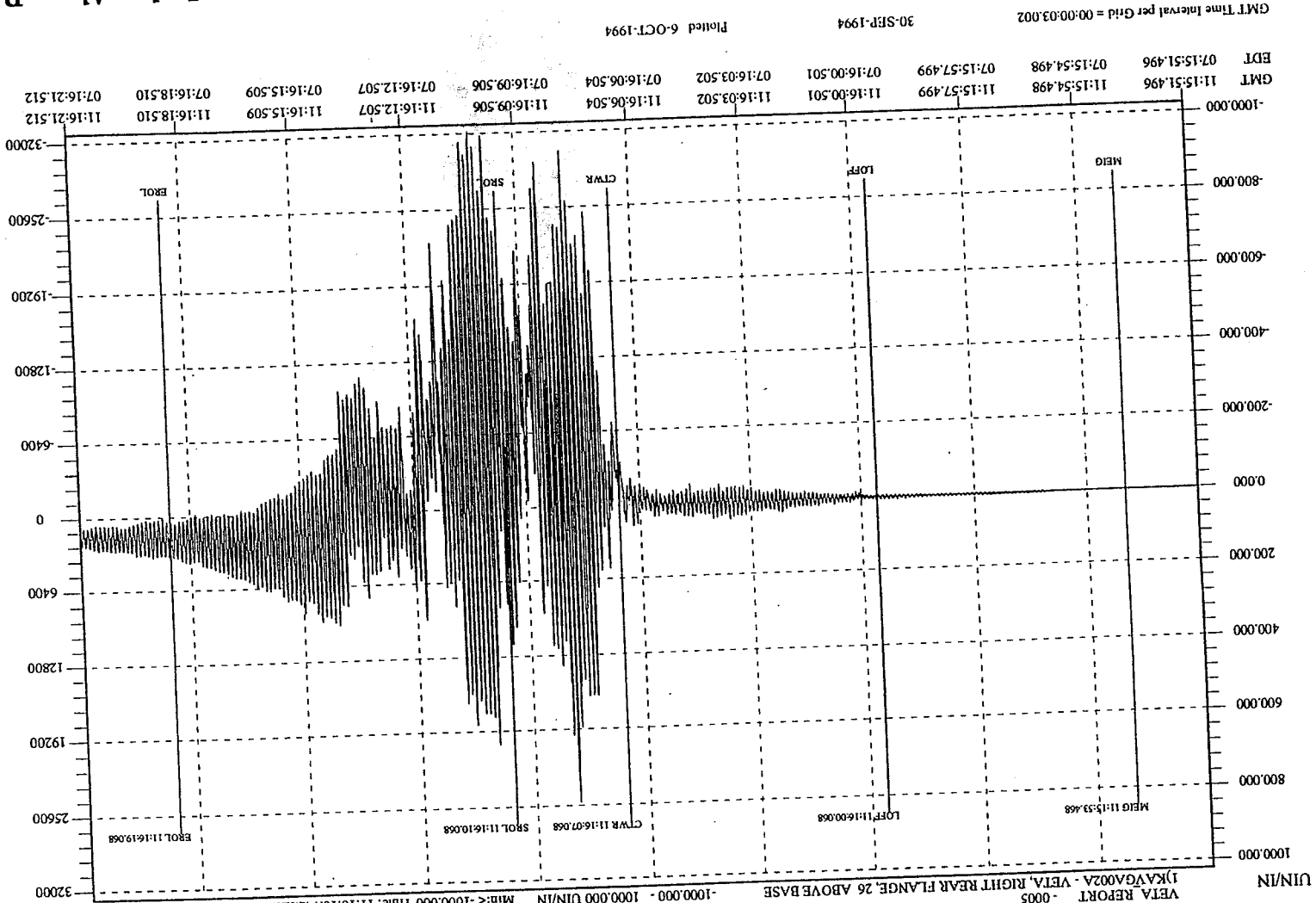


Figure E-2. Strain Response (KAVGA002A) - VETA, Right Rear Flange, 26 Inches Above Bar

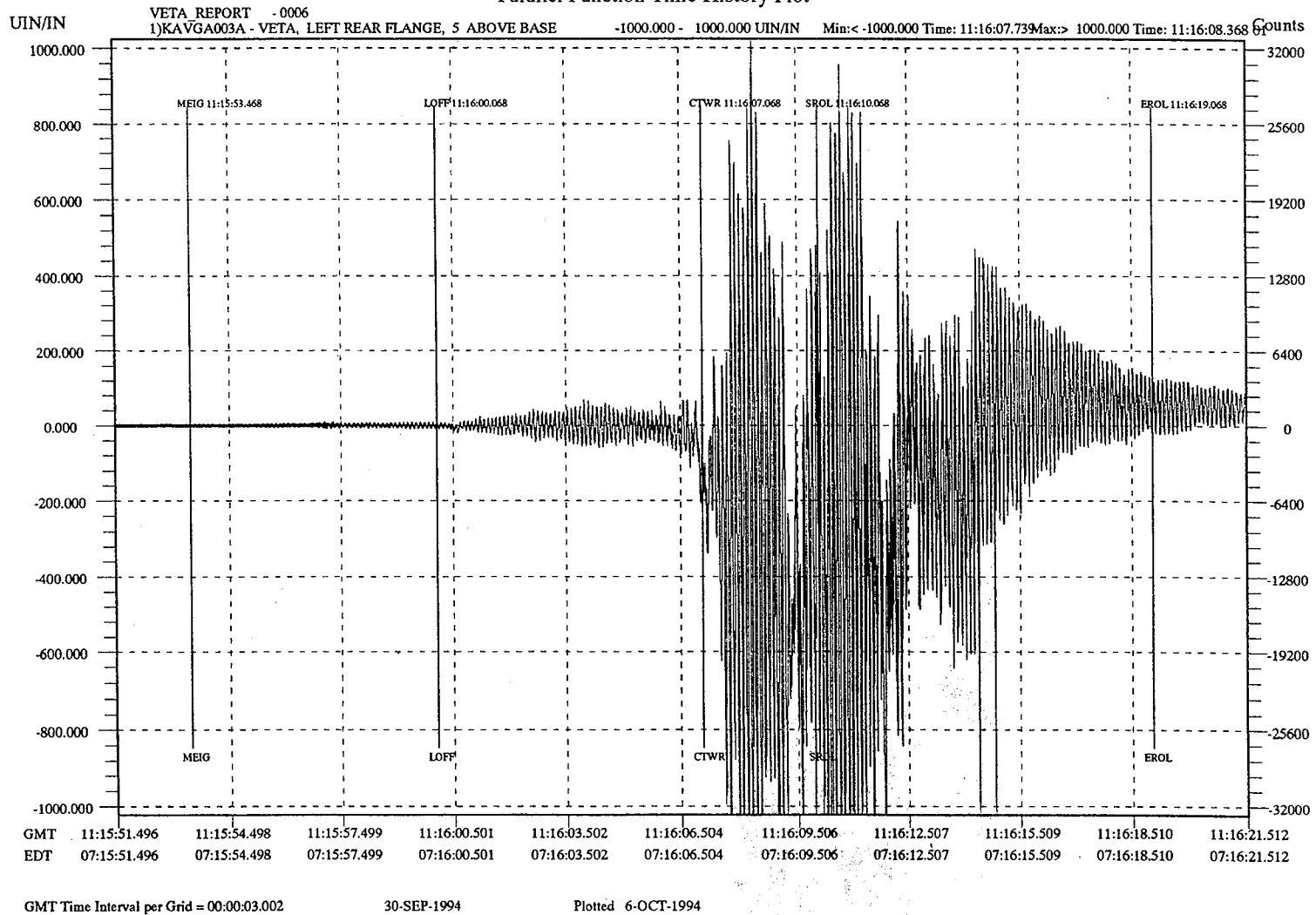


Figure E-3. Strain Response (KAVGA003A) - VETA, Left Rear Flange, 5 Inches Above Base

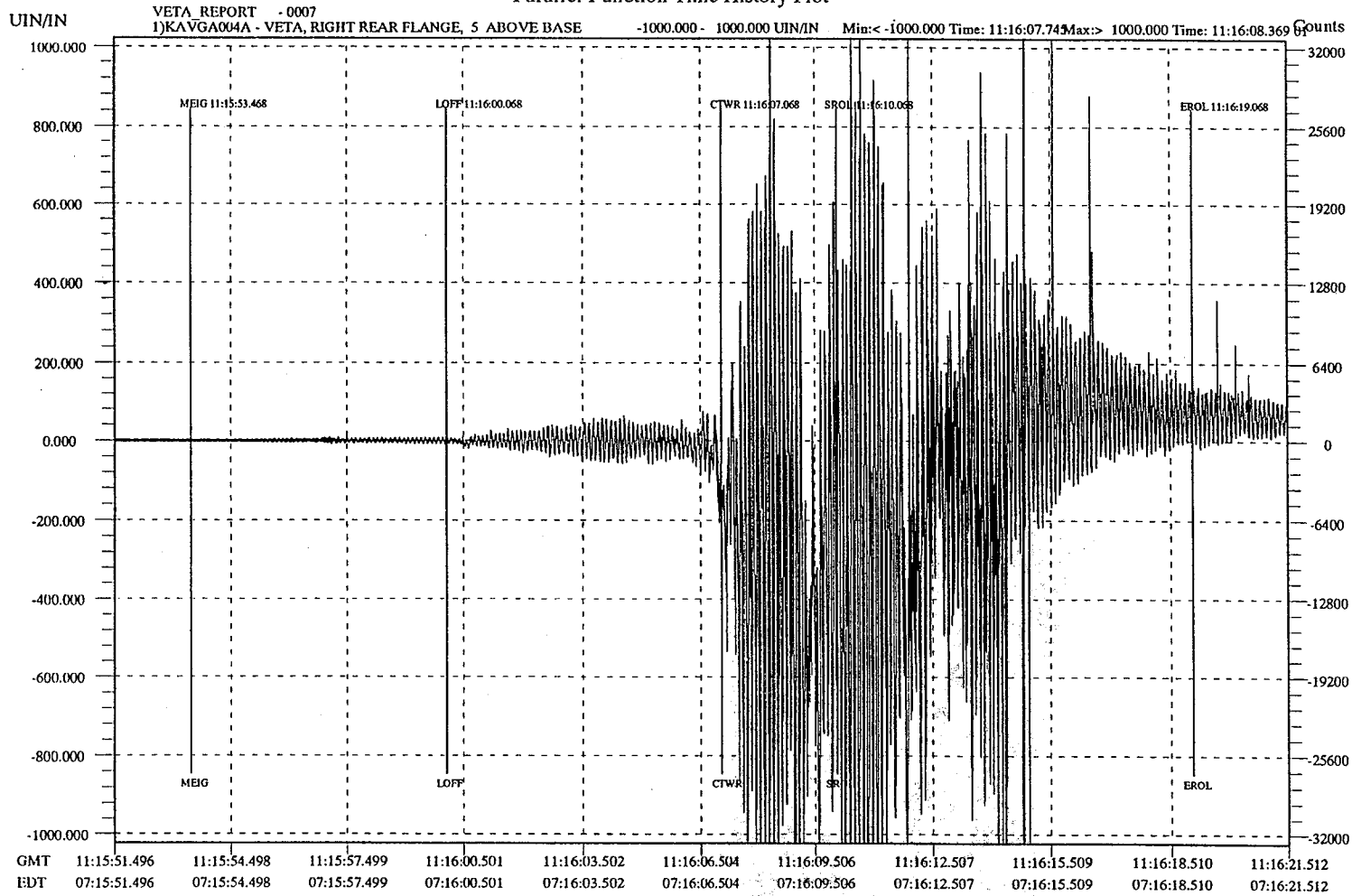


Figure E-4. Strain Response (KAVGA004A) - VETA, Right Rear Flange, 5 Inches Above Base

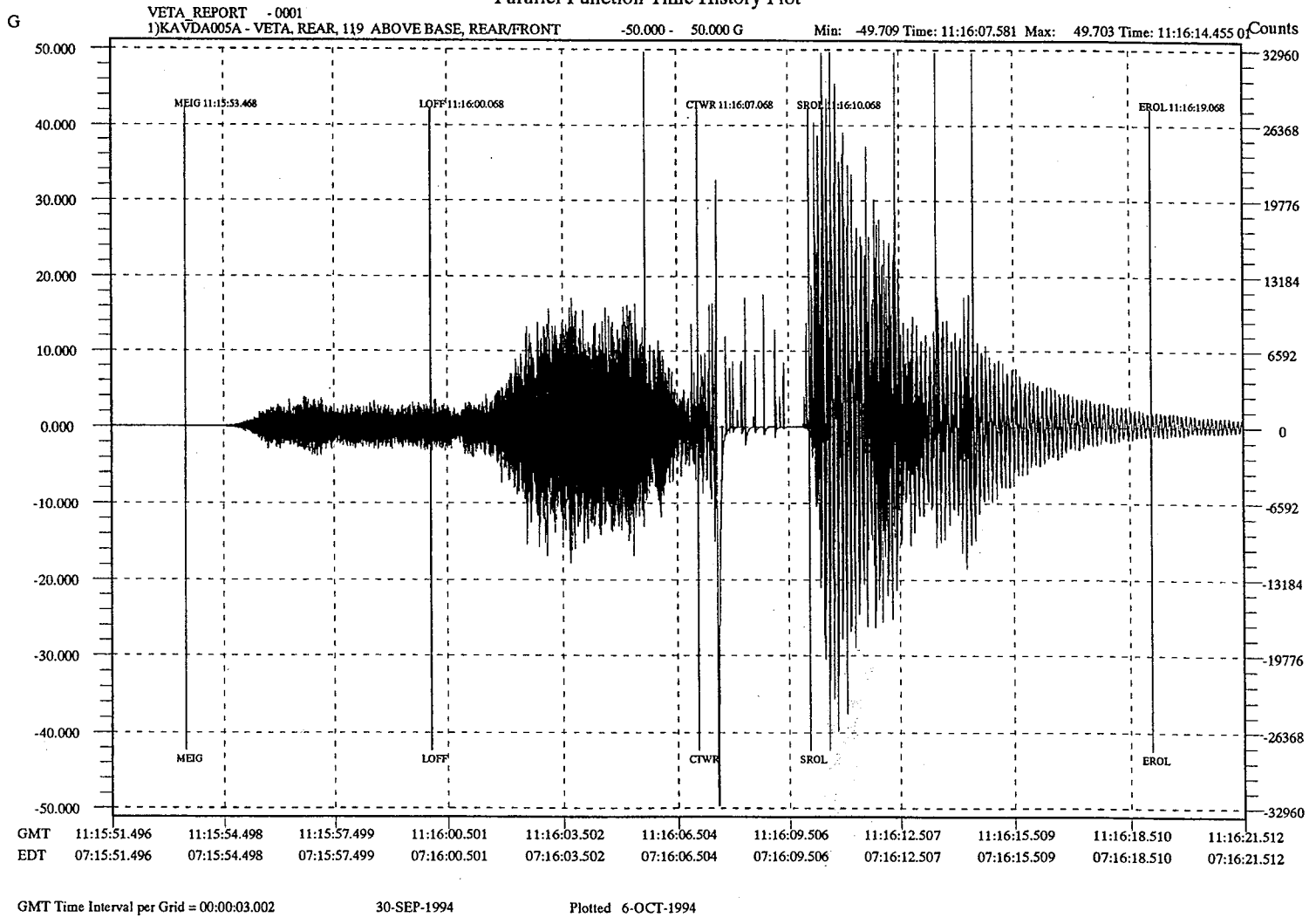


Figure E-5. Acceleration Response (KAVDA005A), VETA, Rear, 119 Inches Above Base

STS-68 LAUNCH S-0007 09/30/94
Parallel Function Time History Plot

VETA REPORT - 0002
1)KAVDA006A - VETA LEFT REAR,61 ABOVE BASE,REAR/FRONT
Min: < -50.000 Time: 11:16:07.580 Max: 41.474 Time: 11:16:10.607 Counts

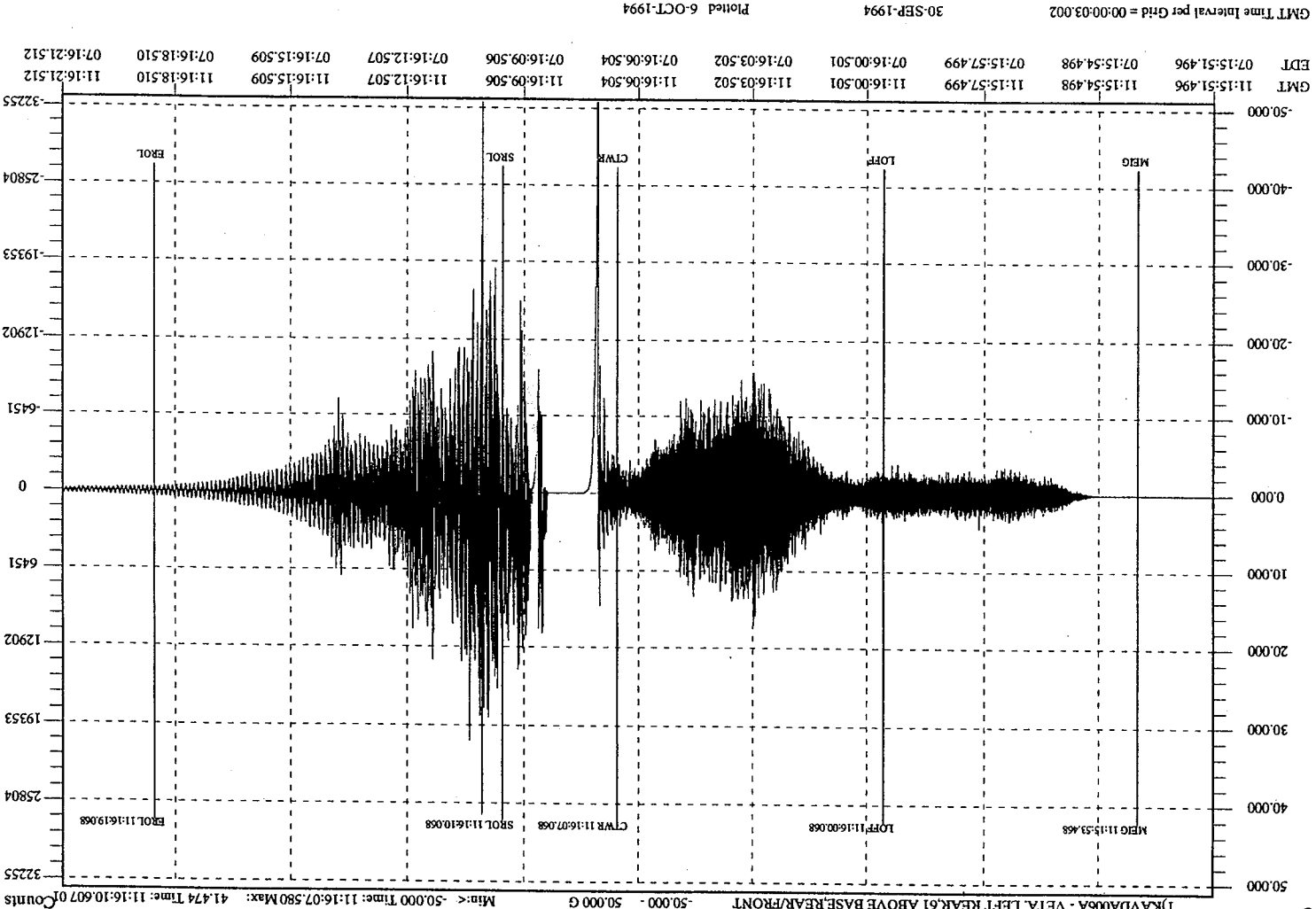
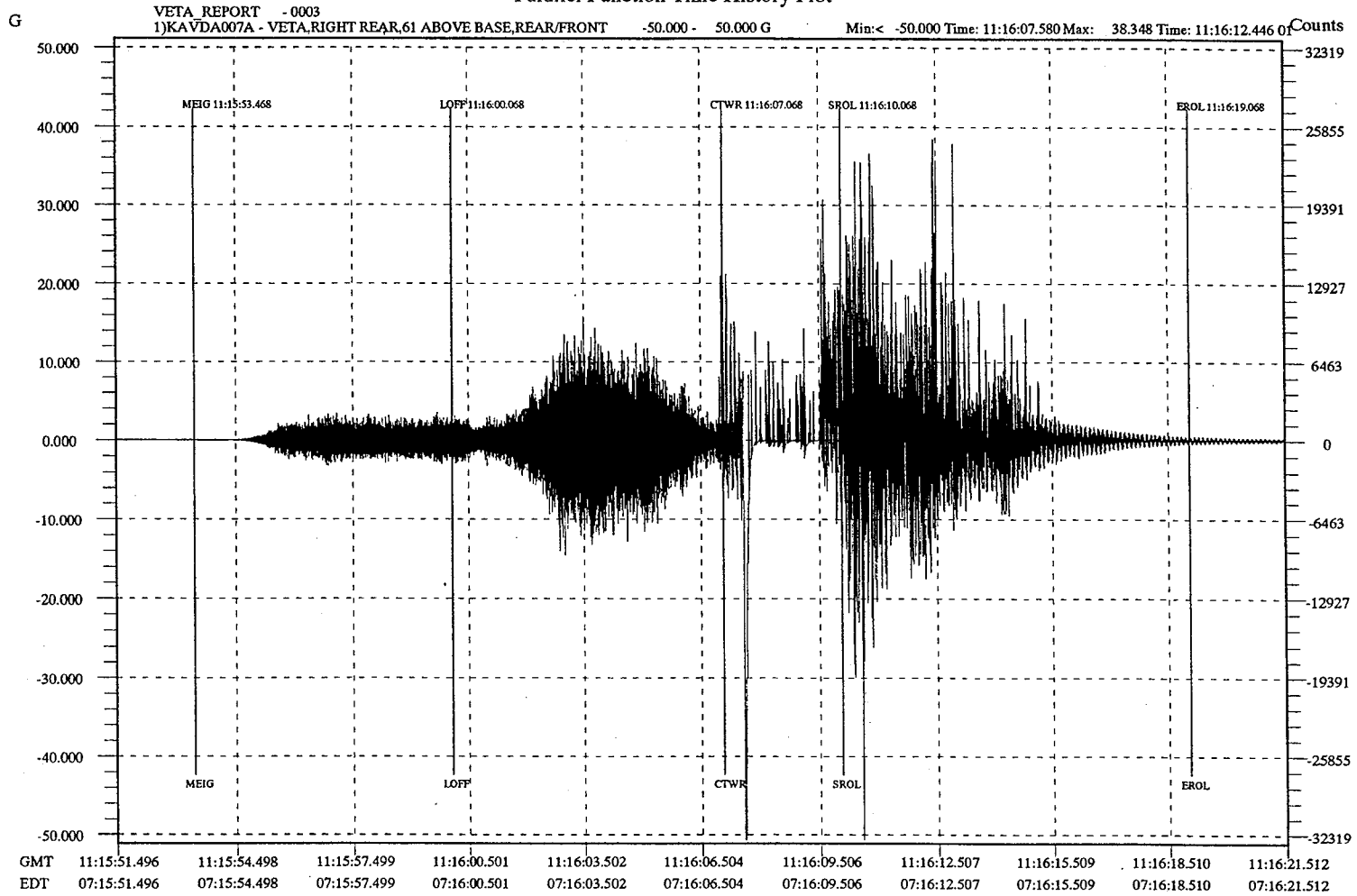


Figure E-6. Acceleration Response (KAVDA006A) - VETA, Left Rear, 61 Inches Above Base



GMT Time Interval per Grid = 00:00:03.002

30-SEP-1994

Plotted 6-OCT-1994

E-9/E-10

Figure E-7. Acceleration Response (KAVDA007A) - VETA, Right Rear, 61 Inches Above Base

APPENDIX F

TEST ANALYSIS CORRELATION

TEST ANALYSIS CORRELATION

A.1 INTRODUCTION

This appendix contains numerical examples illustrating the application of the deterministic approach to compute the response of a cantilever beam. In the examples, the response spectra, pressure correlation lengths, and modal parameters are assumed to be known. The response computations are based on this assumption. Most of the text is devoted to step-by-step explanations of the employed procedure for a sensor distance of 6 feet (see section 9, reference e).

Beam parameters for a cantilever beam are:

Number of spans	$n = 1$
Span length	$l = 127$ inch
Beam width	$b = 14$ inch
Uniform mass	$m = 0.0039837$ lb-sec ² /in ²
Material modulus of elasticity	$E = 29.0 \times 10^6$ pound in ²
Moment of inertia	$I = 9.0433$ in ⁴
Section modulus	$S = I/c = 4.8756$ in ³

A.2 FIRST BENDING MODE

The resonance frequency (undamped) is:

$$f_1 = \frac{0.56}{l^2} \left(\frac{EI}{m} \right)^{1/2} = 8.908 \text{ Hz}$$

$$\omega_1 = 2\pi f_1 = 55.97 \text{ rad/sec}$$

$$\omega_1^2 = 3.132 \times 10^3 \text{ (rad/sec)}^2$$

The generalized modal mass (mode normalized to the maximum unit displacement at the tip) is:

$$M = \frac{1}{2} nml = \frac{1}{2} (1) \left(3.9837 \times 10^{-3} \right) \times 127 = 0.2529 \text{ lb-sec}^2/\text{in}$$

The area exposed to acoustic pressures (for application in the diagrams of K-coefficients) is:

$$A = bl = 14" \times 127" = 1778 \text{ in}^2$$

The response spectrum ordinate for a 1-percent damping (see figure F-1) for the first mode ($f_1 = 8.9$ hertz) is :

$$Y = q/(AJ/M/\omega_1^2) = q \cdot \omega_1^2/(AJ/M) = 2.8$$

This is a maximum value reflecting a 95 percent prediction and confidence limit. Note that the median value is around 2.5. The value chosen above represents the maximum design value.

The pressure correlation length, λ , depends on the direction or orientation of the beam (horizontal or vertical). Computations for the case of a vertical beam (see figure F-2) are:

$$\text{At } f_1 = 8.9 \text{ Hz, } \lambda_v = 19 \text{ feet}$$

The maximum value of J_v (ratio of the generalized modal load by total load) may be computed using two separate programs. It is more applicable to use the C-BEAM program here:

$$\text{Maximum } J_v \text{ computed from C-BEAM program} = 0.347$$

When J_v is known, the following can be computed:

$$AJ_v/M/\omega_1^2 = \frac{1778 \times 0.347}{2529 \times 3.132 \times 10^3} = 0.778$$

The response modal coordinate (modal amplitude or displacement or modal participation factor) is given by:

$$q_{1v} = Y [AJ_v / M/\omega_1^2] = 2.8 (0.478) = 2.178" \text{ at tip}$$

Since the mode was normalized to the maximum unit displacement at the tip, q_{1v} is the maximum tip displacement. This value could be compared with the data from the accelerometer located at the tip for verification..

It should be noted that the modal coordinates q_{1v} and q_{1h} are the multipliers of the first normal mode stress matrix. The stress matrix bending moment is calculated

A:\OTABLE.TXT

Rank 7 Eqn 15 $y=a+b/x^{0.5}$

$r^2=0.79790014$ DF Adj $r^2=0.79584837$ FitStdErr=0.22284303 Fstat=781.71371

$a=3.3857386$

$b=-2.9235183$

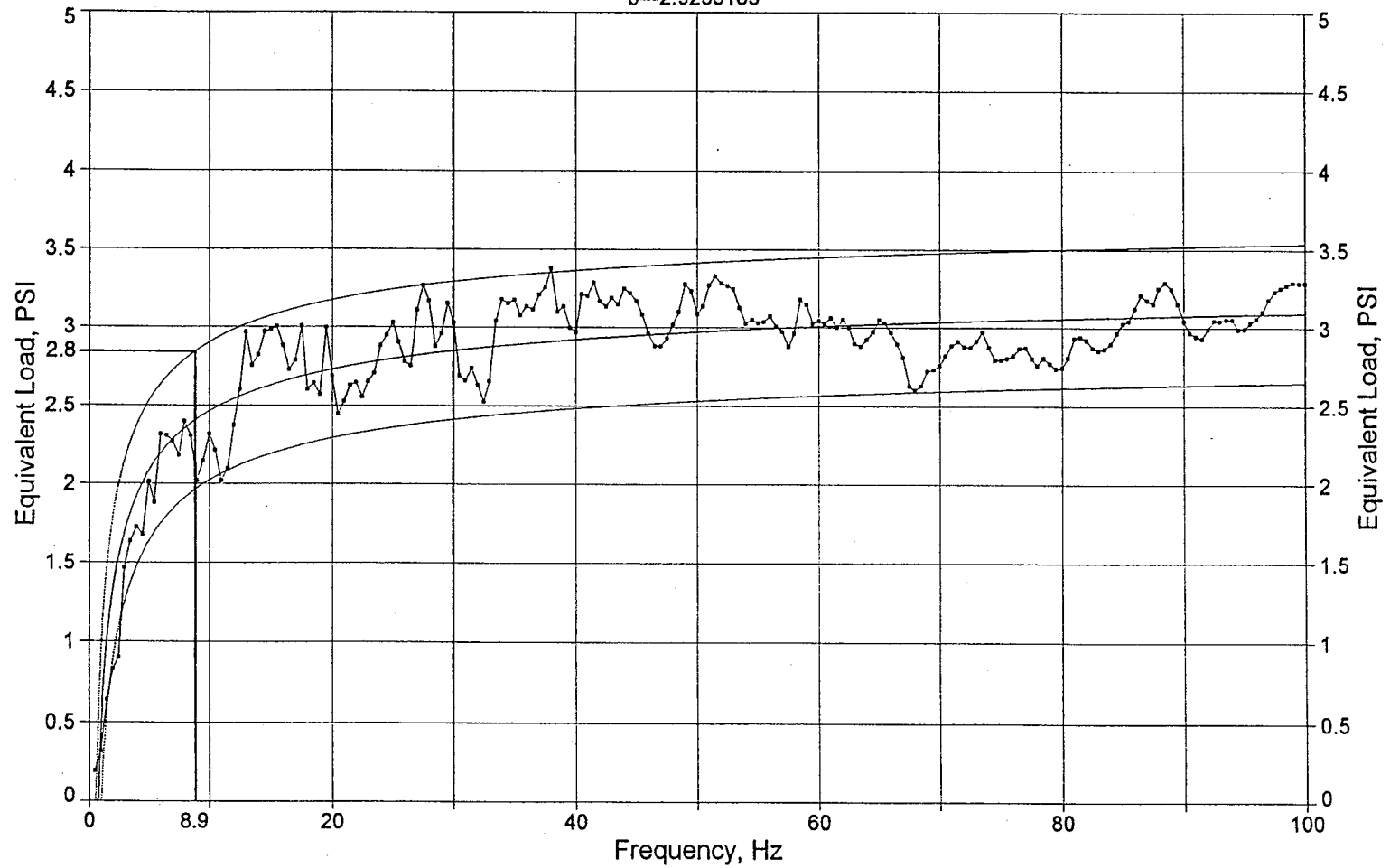


Figure F-1. Response Spectra to Input Pressures
(1 Percent Damping)

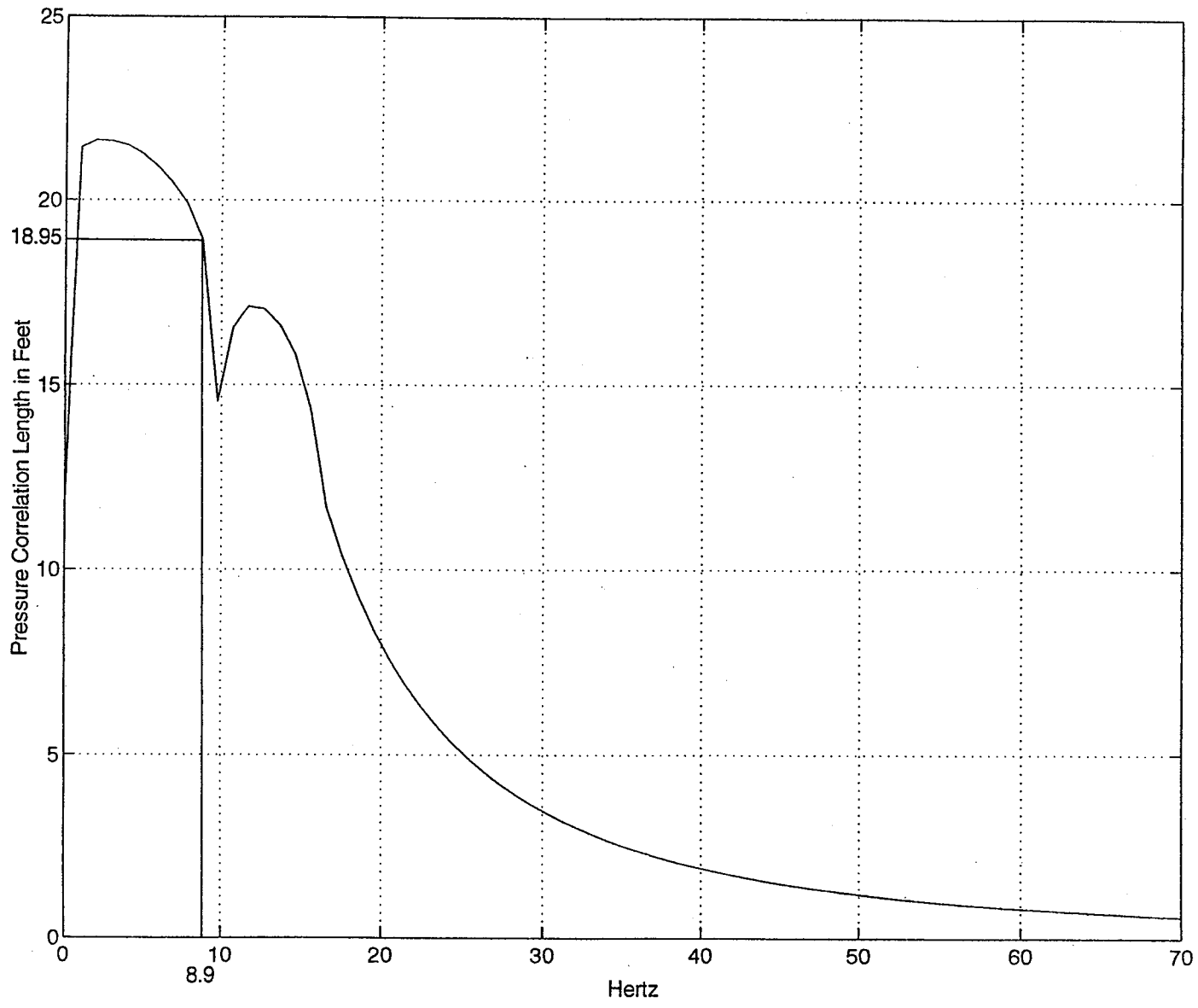


Figure F-2. STS-68, KAVPA004A and KAVPA008A Pressure Correlation Length for 6-Foot Sensor Distance (Front-Back): Net Effective Pressures, Hanned 15X

using the C-BEAM program at the location of the strain gages. The first step of test-analysis correlation involves comparison of predicted and measured strains from the test:

$$M_{b1} \text{ (at } x = 33 \text{ inch)} = 36847 \text{ in}\cdot\text{lb}$$

For a vertical beam, the maximum response bending moment at ($x = 12$ inches) is :

$$\delta M_{rb1v} = q_{1v} \cdot M_{b1} = 2.178 \times 36847 = 80267 \text{ in}\cdot\text{lb}$$

and the maximum stress is:

$$\delta_{rb1v} = \delta M_{rb1v} / S = 80276 / 4.8756 = 16,463 \text{ psi}$$

The predicted strain is:

$$\delta_{ep} = \delta_{rb1v} / E = 16,463 / 29 \times 10^6 = 567''$$

The measured strains during STS-68 launch (see figures F-3 and F-4) at location ($x = 33$ inches) =

$$\frac{516 + 504}{2} = 510 \text{ } \mu\text{in/in}$$

The deviation between predicted and measured is:

$$(\text{predicted} - \text{measured}) / \text{measured} * (100) = (567 - 510) / 510 * 100 = 11.1$$

Similar computation for sensors 3 feet indicated a variation of 5 percent. In general it has been observed that the theory overpredicts by 5 to 10 percent.

Notes

1. The above computations are repeated for at least 3 modes. Since the contribution of the second normal mode was negligible, only the first mode is compared.
2. When higher modes participate, total stress is computed first by squaring and summing stress contribution from each mode and then taking the square root.

3. For the test cantilever, modes were well separated and thus there was no modal coupling.
4. Mode peaks were distinct and sharp, indicating light damping occurred. Actual damping for the first bending mode was 0.45 percent as determined by the modal analysis.

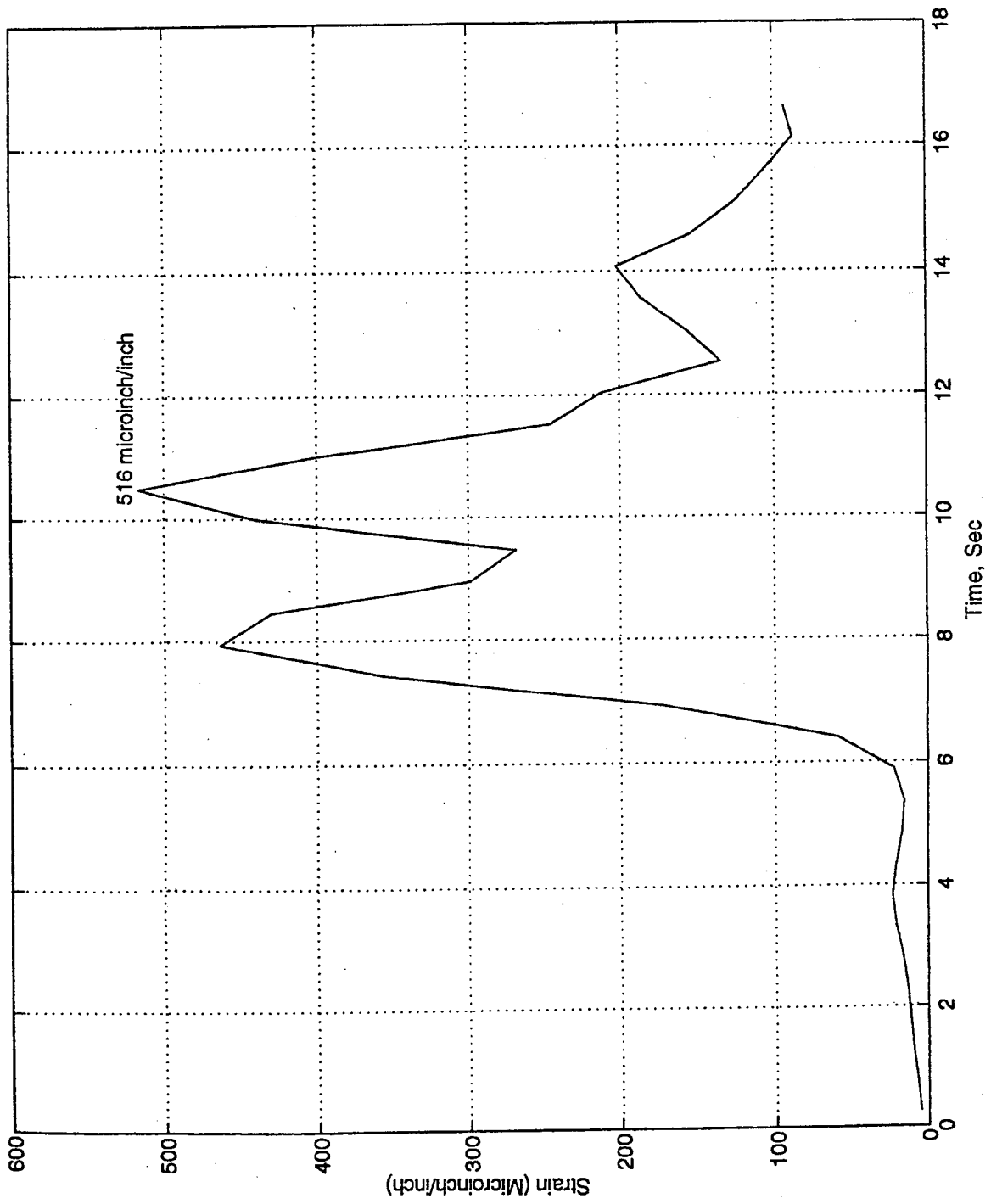
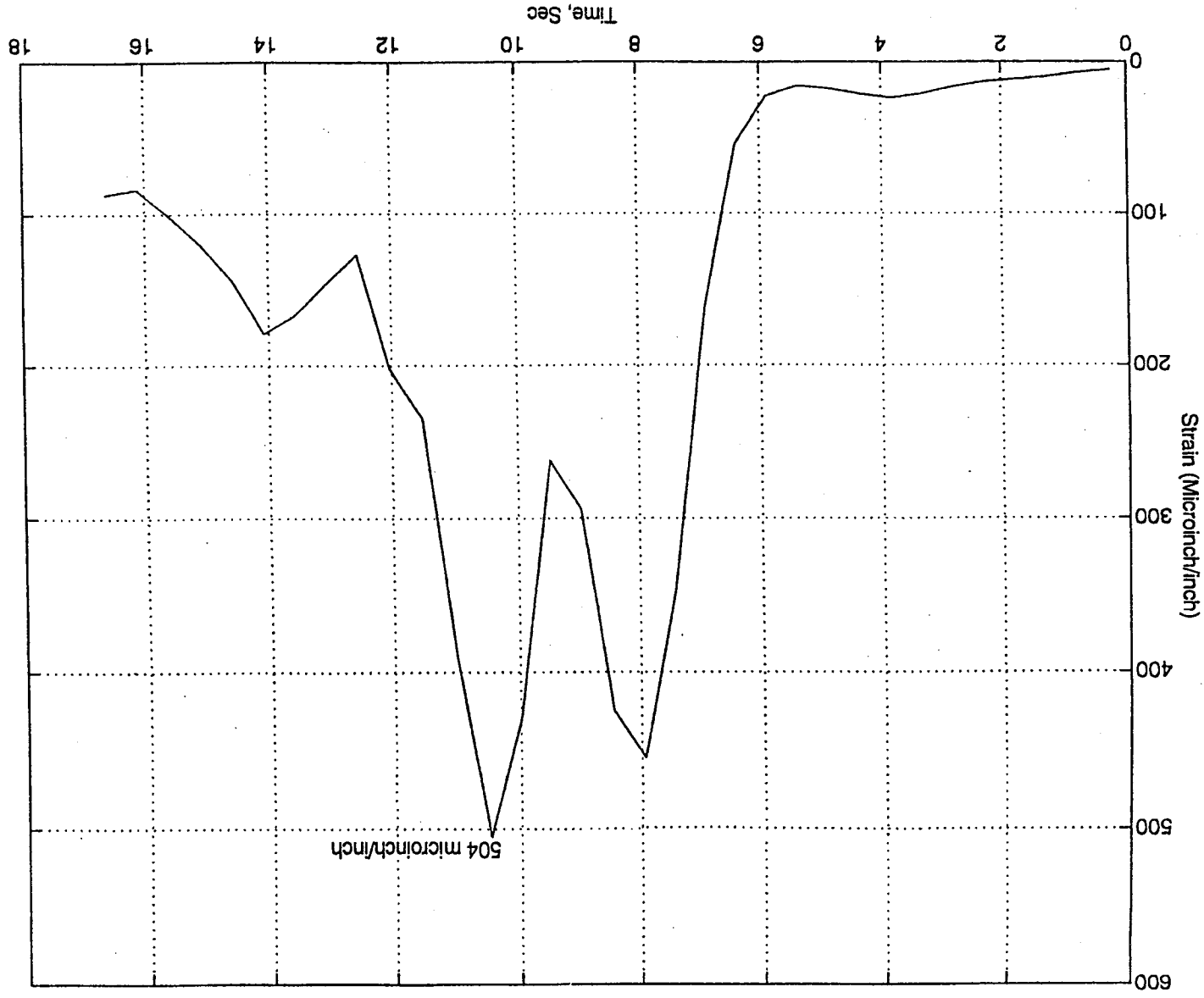


Figure F-3. Strain Response Time History (KAVGA001A)

Figure F-4. Strain Response Time History (KAVGA002A)



REPORT DOCUMENTATION PAGE

Form Approved
OMB No. 0704-0188

Public reporting burden for this collection of information is estimated to average 1 hour per response, including the time for reviewing instructions, searching existing data sources, gathering and maintaining the data needed, and completing and reviewing the collection of information. Send comments regarding this burden estimate or any other aspect of this collection of information, including suggestions for reducing this burden, to Washington Headquarters Services, Directorate for Information Operations and Reports, 1215 Jefferson Davis Highway, Suite 1204, Arlington, VA 22202-4302, and to the Office of Management and Budget, Paperwork Reduction Project (0704-0188), Washington, DC 20503.

1. AGENCY USE ONLY (Leave blank)	2. REPORT DATE April 1997	3. REPORT TYPE AND DATES COVERED Technical Memorandum - 1997	
4. TITLE AND SUBTITLE Validation of a Deterministic Vibroacoustic Response Prediction Model		5. FUNDING NUMBERS	
6. AUTHOR(S) Ravi Margasahayam		8. PERFORMING ORGANIZATION REPORT NUMBER	
7. PERFORMING ORGANIZATION NAME(S) AND ADDRESS(ES) NASA John F. Kennedy Space Center Kennedy Space Center, Florida 32899		10. SPONSORING / MONITORING AGENCY REPORT NUMBER NASA TM-112649	
9. SPONSORING / MONITORING AGENCY NAME(S) AND ADDRESS(ES) National Aeronautics and Space Administration Washington, D.C. 20546		11. SUPPLEMENTARY NOTES Ravi Margasahayam, I-NET Space Services (work funded by NASA Contract NAS 10-11943) Responsible individual: Raoul E. Caimi, DM-ASD, (407)867-3748	
12a. DISTRIBUTION / AVAILABILITY STATEMENT Unclassified - Unlimited Subject Category: This publication is available from the NASA Center for AeroSpace Information, (301)621-0390		12b. DISTRIBUTION CODE	
13. ABSTRACT (Maximum 200 words) This report documents the recently completed effort involving validation of a deterministic theory for the random vibration problem of predicting the response of launch pad structures in the low-frequency range (0 to 50 hertz). Use of the Statistical Energy Analysis (SEA) methods is not suitable in this range. Measurements of launch-induced acoustic loads and subsequent structural response were made on a cantilever beam structure placed in close proximity (200 feet) to the launch pad. Innovative ways of characterizing random, nonstationary, non-Gaussian acoustics are used for the development of a structure's excitation model. Extremely good correlation was obtained between analytically computed responses and those measured on the cantilever beam. Additional tests are recommended to bound the problem to account for variations in launch trajectory and inclination.			
14. SUBJECT TERMS random vibration, vibroacoustics, and nonstationary loads			15. NUMBER OF PAGES
17. SECURITY CLASSIFICATION OF REPORT Unclassified			16. PRICE CODE
18. SECURITY CLASSIFICATION OF THIS PAGE Unclassified	19. SECURITY CLASSIFICATION OF ABSTRACT Unclassified	20. LIMITATION OF ABSTRACT	